Journal of Medicinal Chemistry

Article

pubs.acs.org/jmc

In Vivo Phenotypic Screening for Treating Chronic Neuropathic Pain: Modification of *C*2-Arylethynyl Group of Conformationally Constrained A_3 Adenosine Receptor Agonists

Dilip K. Tosh,[†] Amanda Finley,[§] Silvia Paoletta,[†] Steven M. Moss,[†] Zhan-Guo Gao,[†] Elizabeth T. Gizewski,[‡] John A. Auchampach,[‡] Daniela Salvemini,[§] and Kenneth A. Jacobson*,[†]

[†]Molecular Recognition Section, Laboratory of Bioorganic Chemistry, National Institute of Diabetes and Digestive and Kidney Diseases, National Institutes of Health, Building 8A, Room B1A-19, Bethesda, Maryland 20892-0810, United States

[‡]Department of Pharmacology, Medical College of Wisconsin, 8701 Watertown Plank Road, Milwaukee, Wisconsin 53226, United States

[§]Department of Pharmacological and Physiological Science, Saint Louis University School of Medicine, St. Louis, Missouri 63104, United States

S *Supporting Information*

ABSTRACT: (N)-Methanocarba adenosine 5′-methyluronamides containing 2-arylethynyl groups were synthesized as A_3 adenosine receptor (AR) agonists and screened in vivo (po) for reduction of neuropathic pain. A small N^6-methyl group maintained binding affinity, with human > mouse A_3AR and MW < 500 and other favorable physicochemical properties. E_{max} (maximal efficacy in a mouse chronic constriction injury pain model) of previously characterized A_3AR agonist, 2-(3,4-difluorophenylethynyl)-N^6-(3-chlorobenzyl) derivative **6a**, MRS5698, was surpassed. More efficacious analogues (in vivo) contained the following *C*2-arylethynyl groups: pyrazin-2-yl **23** (binding K_i, hA_3AR, nM 1.8), fur-2-yl **27** (0.6), thien-2-yl **32** (0.6) and its 5-chloro **33**, MRS5980 (0.7) and 5-bromo **34** (0.4) equivalents, and physiologically unstable ferrocene **36**, MRS5979 (2.7). **33** and **36** displayed particularly long in vivo duration (>3 h). Selected analogues were docked to an A_3AR homology model to explore the environment of receptor-bound *C*2 and N^6 groups. Various analogues bound with μM affinity at off-target biogenic amine (M_2, $5HT_{2A}$, β_3, $5HT_{2B}$, $5HT_{2C}$, and α_{2C}) or other receptors. Thus, we have expanded the structural range of orally active A_3AR agonists for chronic pain treatment.

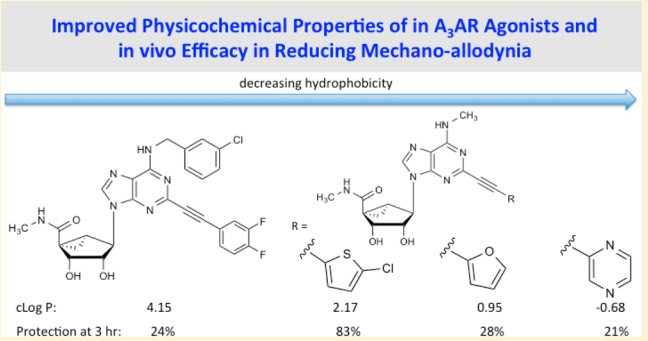

INTRODUCTION

Chronic neuropathic pain (NP) is a widespread condition that is often associated with diabetes, cancer, injury, exposure to toxic substances, and a variety of other diseases.[1,2] When it occurs subsequent to cancer chemotherapy, it often necessitates the discontinuation of a life-saving treatment. The currently used therapies for NP are poorly efficacious and suffer from serious side effects, ranging from liver toxicity to addiction and personality changes. In many cases, the therapy involves drugs developed for a different condition that were incidentally found to reduce NP, e.g., biogenic amine reuptake inhibitors such as the antidepressant amitriptyline or anticonvulsant drugs such as gabapentin. Opioids, which are effective against acute pain, are not the first line of treatment for chronic NP, both because of addiction liability and low efficacy.[3] Thus, there is an unsolved medical need for chronic neuropathic pain treatment that necessitates the exploration of novel mechanisms, such as purinergic therapy by agonists of adenosine receptors (ARs), inhibitors of adenosine kinase, and modulators of nucleotidases.[4,5] The A_3 subtype of the ARs (A_3AR) is expressed in low levels in many tissues and cell types, including neurons and glial cells, and has recently become a promising target for treating NP.[6−8]

A_3AR agonists, such as nucleosides **1**−**5** (Chart 1), are efficacious in models of inflammatory disease, cancer, stroke, cardiac ischemia, and other conditions.[9] Prototypical A_3AR agonists, ribosides N^6-(3-iodobenzyl)-5′-*N*-methylcarboxamidoadenosine (IB-MECA, **1**) and its 2-chloro analogue **2** and thioriboside **3** are efficacious in vivo.[10−12] Prototypical agonists **1** and **2** are advancing to phase II and III clinical trials for psoriasis, rheumatoid arthritis, and hepatocellular carcinoma.[13,14] A_3AR agonists **4** and **5** additionally have a conformationally rigid ribose substitution consisting of a bicyclo[3.1.0]hexane (methanocarba) ring system that maintains a receptor-preferred North (N) conformation. A_3AR agonists of general structure **6** furthermore contain a rigid *C*2-phenylethynyl extension that enhances selectivity, especially in the (N)-methanocarba series. Compounds **1**, **2**, and **4** were shown to be active in reducing or preventing the development of

Received: July 7, 2014
Published: November 25, 2014

Chart 1. Prototypical A_3AR Agonists in the Ribo (1, 2), Thioribo (3), and (N)-Methanocarba (4, 5) Series, Including Design Features of New Derivatives As Indicated with General Structure 6

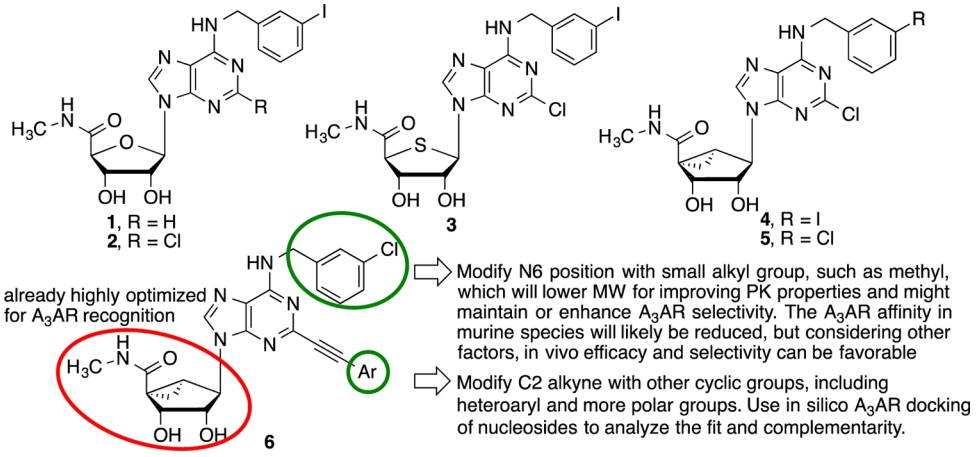

mechanically- and chemotherapy-induced NP in mice and rats.[10] The specific example of **6a** in which Ar is 3,4-difluorophenyl was also shown to be effective in in vivo models of NP.[15] These selective nucleoside A_3AR agonists potently and dose dependently reduce chronic NP and also augment the effects of commonly used agents for this condition, such as opiates. A_3AR agonists reduce the NP associated with administration of various chemotherapeutic agents representing three different mechanisms of anticancer action.[10,15,16]

Although agonists of the A_1 and A_{2A}ARs also have analgesic properties, they additionally have potent cardiovascular side effects such as changes in heart rate and blood pressure,[4,17−19] which are not as strongly associated with the activation of the A_3AR.[20,21] Thus, we seek orally bioavailable and highly selective A_3AR agonists that have activity against chronic NP of distinct etiologies.[10] We have approached this problem by designing and synthesizing new analogues of our previously reported chemical class of 2-alkynyl-(N)-methanocarba adenosine 5′-methyluronamides[22] that might display improved and more drug-like physicochemical properties than previous agents. There are both peripheral and central mechanistic components to the observed protection against NP by A_3AR agonists.[11] Thus, the ability to cross the blood−brain barrier as well as oral bioavailability would be desirable in a clinical candidate.

The 2-phenylethynyl groups that we previously reported to enhance the selectivity of (N)-methanocarba adenosine derivatives as A_3AR agonists are the focus of this structure−activity relationship (SAR) study.[15] The current strategy is to expand structurally the family of A_3AR agonists for treatment of NP and other diseases. As shown in Chart 1, in this study ring structures appended to the 2-ethynyl group were varied to encompass diverse heterocyclic and other aryl groups and cycloalkyl groups. The reference compound **6a** is highly efficacious in reversing chronic NP,[6,22] but it has nonoptimal physicochemical properties (lipophilicity and MW) for drug development. Therefore, a group frequently included at the N^6 position of A_3AR agonists, N^6-(3-halobenzyl), was replaced with a smaller N^6-methyl group, which we already demonstrated to maintain human (h) A_3AR binding affinity in this chemical series.[22] A beneficial effect of the N^6-methyl substitution was to reduce the molecular weight to below 500, which brings the analogues in closer compliance to Lipinski's guidelines for bioavailable compounds.[23] There was a cost associated with this structural shift, i.e., a species difference in receptor affinity, which was decreased at the mouse (m) A_3AR in comparison to the hA_3AR.[11] Nevertheless, when administered po in mice, these derivatives consistently displayed in vivo activity reflective of A_3AR activation, with varying degrees of efficacy at a single dose.

We have used an in vivo phenotypic drug discovery (PDD) screen that reflects both pharmacokinetic and pharmacodynamics factors to demonstrate oral bioavailability and high efficacy of several of the newly synthesized nucleoside analogues. The pharmaceutical industry is rediscovering the predictive value of physiology-based PDD strategies.[24] The initial screening used was the Bennett mouse model of chronic neuropathic pain resulting from constriction injury (CCI) of the sciatic nerve,[25] in which the compound was administered by oral gavage (po) rather than intraperitoneally (ip), as we reported in earlier studies of A_3AR agonists in the same model.[10] Although the expectation of A_3AR selectivity of the newly synthesized analogues was high based on existing SAR, they were additionally subjected to measurement of their AR interactions. Binding and functional assays at the heterologously expressed h and m ARs were performed, as well as screening of selected compounds at off-target sites.[26] The A_3AR is a G protein-coupled receptor (GPCR) of the rhodopsin-like family A and as such is amenable to molecular modeling based on homology to closely related GPCRs,[11,15] specifically the structures of the agonist-bound active-like $A_{2A}AR$.[27,28] Novel structures that were efficacious in vivo and bound potently to the receptor were docked to an A_3AR homology model. Thus, in vitro pharmacology and molecular modeling were used to help interpret the positive in vivo results obtained for promising analogues.

RESULTS

The novel (N)-methanocarba adenosine analogues **14**−**18** and **20**−**38** (Table 1) were synthesized and tested in a phenotypic screen as described below. Charged compounds were not included because they might be impaired in the ability to cross the blood−brain barrier.[9] Related previously reported reference compounds[22] included in Table 1 are N^6-(3-chlorobenzyl)-3,4-difluorophenyl **6a**, N^6-methyl-*C*2- halophenylethynyl **8**−**13** and simple phenyl **7a**, biphenyl **7b**, and 2-pyridyl **19** analogues. The new nucleosides are all N^6-methyl compounds, for which the *C*2 substituent consists of the following substituted ethynyl groups: phenyl **14**−**18**, nitrogen heterocycle **19**−**26**, furan **27**−**30**, thiophene **31**−**35**, ferrocene ($Fe(C_5H_5)_2$) **36**, and cycloalkyl **37** and **38**. For comparison with the new analogues, structures and

dx.doi.org/10.1021/jm501021n | J. Med. Chem. 2014, 57, 9901−9914

Table 1. Structures and Binding Affinities of Newly Synthesized AR Agonists (14−18 and 20−38) and Reference Compounds (6a−13 and 19)[a]

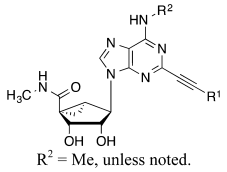

R^2 = Me, unless noted.

Compd.	R^1	hA_1AR[c] % inhibition	$hA_{2A}AR$[c] % inhibition	A_3AR[c] or K_i (nM)
6a[b] R^2 = 3-chlorobenzyl	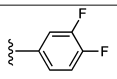	*6% ± 4%, 16% ± 3% (m)*	*41% ± 10%, 27% ± 2% (m)*	3.49±1.84, 3.08±0.23 (m)
7a[b]		*18% ± 8%*	*14% ± 7%*	0.85±0.22
7b[b]	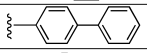	*18% ± 8%*	*21% ± 6%*	3.10±1.26
8[b]		*20% ± 7%*	*17% ± 2%*	0.97±0.38
9[b]		*14% ± 2%*	*10% ± 5%*	0.97±0.24
10[b]	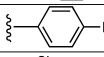	*27% ± 17%*	*19% ± 3%*	0.53±0.09, 37.7±1.1 (m)
11[b]		*22% ± 6%*	*30% ± 5%*	0.58±0.04, 37.2±2.0 (m)
12[b]	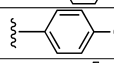	*13% ± 1%*	*30% ± 1%*	1.22±0.31
13[b]		*6% ± 6%*	*6% ± 6%*	1.65±0.08, 86±6 (m)
14		*12 ± 7%*	*20 ± 7%*	0.77±0.17
15	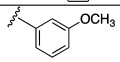	*8 ± 4%*	*26 ± 5%*	0.91±0.07
16	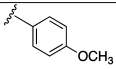	*10 ± 5%*	*24 ± 8%*	0.63±0.07
17	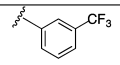	*10 ± 9%*	*12 ± 6%*	3.39±0.65
18	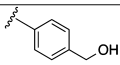	*16 ± 6%*	*11 ± 7%*	2.16 ± 0.39
19[b]		*13% ± 8%*	*13% ± 4%*	1.01±0.36, 58.2 ± 3.6 (m)
20		*16 ± 10%*	*12 ± 6%*	2.15±0.38
21		*15 ± 3%*	*2 ± 2 %*	2.07 ± 0.16
22		*25 ± 10%*	*27 ± 5%*	1.97 ± 0.27, 65±6 (m)
23		*37 ± 6%, 57% ± 2% (m)*	*25 ± 9%, 12% ± 5% (m)*	1.76 ± 0.22, 68±5 (m)
24		*11 ± 3%*	*13 ± 8%*	3.53 ± 0.99, 112±10 (m)
25		*30 ± 2%*	*19 ± 2%*	2.23 ± 0.18, 50±2 (m)
26	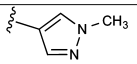	*35 ± 7%, 72% ± 6% (m)*	*12 ± 6%, 16% ± 2% (m)*	2.34±0.29, 126±30 (m)
27		*30 ± 1%, 59% ± 2% (m)*	*18 ± 9%, 17% ± 1% (m)*	0.62±0.06, 54±11 (m)
28	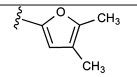	*15 ± 6%*	*21 ± 3%*	1.45 ± 0.20
29	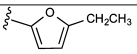	*18 ± 9%*	*4 ± 4%*	1.50 ± 0.28
30	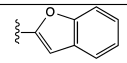	*13 ± 3%*	*18 ± 3%*	1.62 ± 0.23
31		*11 ± 6%*	*3 ± 2%*	0.52±0.04
32		*25 ± 5%, 47% ± 2% (m)*	*20 ± 6%, 3% ± 3% (m)*	0.57 ± 0.10, 43±2 (m)
33	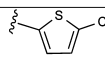	*6 ± 1%, 38% ± 2% (m)*	*24 ± 13%, 7% ± 3% (m)*	0.70 ± 0.11, 36.1±4.7 (m)
34	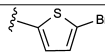	*18 ± 5%*	*19 ± 3%, 10% ± 3% (m)*	0.44 ± 0.12
35		*31 ± 11%*	*8 ± 5%*	2.10 ± 0.37
36	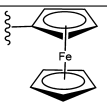	*25 ± 2%, 45% ± 2% (m)*	*47 ± 2%, 4% ± 2% (m)*	2.68 ± 0.44, 5.46±0.67 (m)
37		*38 ± 6%*	*15 ± 10%*	1.15 ± 0.18
38		*15 ± 5%*	*45 ± 6%*	1.68±0.60, 40.9±1.9 (m)

[a]Binding in membranes prepared from CHO or HEK293 (A_{2A} only) cells stably expressing one of three hAR subtypes. The binding affinity for hA_1, A_{2A}, and A_3ARs was expressed as K_i values (n = 3−4), measured using agonist radioligands [^{3}H]N^6-*R*-phenylisopropyladenosine **65**, [^{3}H]2-[*p*-(2-carboxyethyl)phenyl-ethylamino]-5′-*N*-ethylcarboxamido-adenosine **66**, or [^{125}I]N^6-(4-amino-3-iodobenzyl)adenosine-5′-*N*-methyl-uronamide **67**, respectively. A percent in italics refers to inhibition of binding at 10 μM. Nonspecific binding was determined using **68** (10 μM at hARs, 100 μM at mARs). [b]Compounds **6a−13** and **19** were reported earlier in Tosh et al.[22] [c]Human, unless noted (m). Binding in membranes prepared from HEK293 cells stably expressing the mA_3AR. Radioligand used was [^{125}I]N^6-(4-amino-3-iodobenzyl)adenosine-5′-*N*-methyl-uronamide **67**. The data (n = 3−4) are expressed as K_i values. A percent in italics refers to inhibition of binding at 10 μM.

binding affinities of previously reported potent A_3AR agonists are provided.

The synthetic methods (Scheme 1) followed the route reported earlier starting with L-ribose.[11,22,29] 6-Chloro 5′-ethyl ester intermediate **39** was treated with five equivalents of methylamine hydrochloride in the presence of triethylamine followed by a 40% methylamine solution (aqueous) at room temperature to provide intermediate 2-iodo 5′-methylamide **40**

dx.doi.org/10.1021/jm501021n | J. Med. Chem. 2014, 57, 9901−9914

Scheme 1. Synthesis of N^6-Methyl (N)-Methanocarba Derivatives[a]

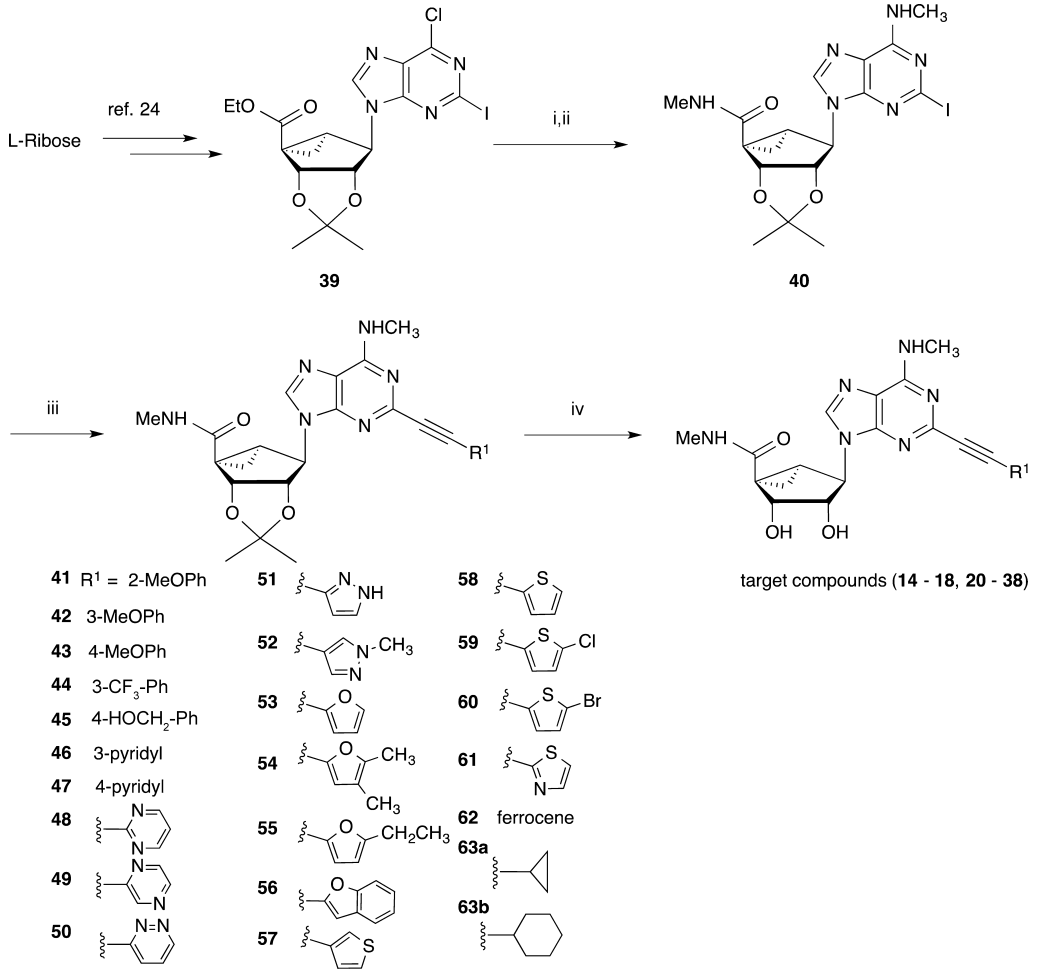

[a]Reagents: (i) $MeNH_2$·HCl, Et_3N, MeOH; (ii) 40% $MeNH_2$, MeOH, rt; (iii) HC≡CR^1, $Pd(PPh_3)_2Cl_2$, CuI, Et_3N, DMF, rt; (iv) 10% TFA, MeOH, 70 °C.

for the N^6-methyl derivatives. Then, **40** was subjected to Sonogashira coupling with the appropriate aryl- or cycloalkylacetylene in the presence of $PdCl_2(Ph_3P)_2$, CuI, and triethylamine to give protected intermediates **41**−**63**. Finally, hydrolysis of the 2′,3′-isopropylidene protecting group afforded the nucleoside target compounds **14**−**18** and **20**−**38** for biological testing.

The N^6-methyl (N)-methanocarba derivatives were tested in mice for the ability to reverse the development of neuropathic pain in a standard model of CCI.[25] Each nucleoside was administered orally (po) at the time peak pain was reached, i.e., on day 7 following constriction of the sciatic nerve. Measurements of paw withdrawl threshold (value in g increases with pain protection) were made between 30 min and 5 h post drug. The results indicating maximal protective effect (E_{max} as a percentage of complete reversal at peak protection) at a standard dose (3 μmol/kg, roughly 1.2−1.6 mg/kg) and its duration (based on the efficacy remaining at 3 h) are presented in Table 2, and time curves at three doses for three selected compounds that achieved near maximal reversal of NP are shown in Figure 1. However, previously reported halogenated *C*2-phenylethynyl derivatives[22] **8**−**12** did not reach full reversal of NP (40−72% efficacy), but a 3,4-difluoro analogue **13** was fully efficacious. Methoxyphenyl- (**14**−**16**, with the *o*-isomer **14** having the highest efficacy), 3-trifluoromethyl- **17**, and 4-hydroxymethyl-phenyl **18** derivatives did not exceed that range. All of the pyridyl derivatives (**19**−**21**) were of low efficacy (29−41%). A 2-(pyrimidin-2-yl)ethynyl analogue **22**, 2-(pyrazin-2-yl)ethynyl analogue **23**, 2-(*N*-methylpyrazol-2-yl)ethynyl analogue **26**, 2-(fur-2-yl)ethynyl analogue **27**, 2-(benzofur-2-yl)ethynyl analogue **30**, 2-(thien-2-yl)ethynyl analogue **32**, 2-(5-chlorothien-2-yl)ethynyl derivative **33** and its 5-Br analogue **34**, and an unusual organometallic (ferrocene) derivative **36** were among the most efficacious in the CCI model with E_{max} in the range of 87−100%. This protection exceeded that produced by a previously characterized A_3AR agonist,[15,22] 2-(3,4-difluorophenylethynyl)-N^6-3-chlorobenzyl derivative **6a** administered po. Thiazole analogue **35** was much less effective in vivo than the structurally similar thiophene **32**.

The duration was indicated by the % protection remaining at the 3 h time point. The duration of effect of 5-chlorothienyl derivative **33** and ferrocene derivative **36** appeared to be longer than for the other analogues, with approximately 80% protection remaining at 3 h. The effects of compounds **30** and **34** were also long lasting, with roughly half of the peak efficacy remaining at 3 h. Thus, on the basis of either in vivo E_{max} or duration, the most favorable of the new compounds for in vivo application were **23** (K_i at hA_3AR, nM 1.8), **27** (0.6), **32** (0.6), **33** (0.7), **34** (0.4), and **36** (2.7). According to the dose−response relationship in Figure 1, **33** (intermediate dose of 0.46 mg/kg producing ∼80% reversal) was more potent in vivo than **23** and **27**.

The nucleoside derivatives were secondarily tested in standard radioligand binding assays at three hAR subtypes (Table 1) to confirm A_3AR selectivity.[11,22] The hA_1AR and hA_3AR were stably

dx.doi.org/10.1021/jm501021n | J. Med. Chem. 2014, 57, 9901−9914

Table 2. Activity of Orally Administered AR Agonists (3 μmol/kg) in CCI Model of Neuropathic Pain in Mice and Physicochemical Parameters

compd	time of peak protection (h)	max effect E_{max} (% ± SEM)[a]	effect at 3 h (% ± SEM)	MW (D)	cLogP[b]	tPSA (Å^2)
N^6-(3-Halobenzyl) Derivatives (Reference) Compounds						
1	1	94.1 ± 5.9	38.7 ± 3.1	510	0.48	131
2	ND[c]	ND	ND	544	1.20	131
6a	1	100 ± 0.0	23.7 ± 10.8	565	4.15	122
N^6-Methyl Derivatives						
7a	0.5−1	44.1 ± 9.9	5.0 ± 5.0	418	1.77	122
7b	1	57.7 ± 9.0	14.3 ± 14.3	495	3.66	122
8	0.5	56 ± 12.5	9.8 ± 16.7	436	1.92	122
9	1−2	46.3 ± 6.3	12.4 ± 3.4	436	1.96	122
10	1−2	72 ± 21.2	10.4 ± 10.4	436	1.92	122
11	0.5	27.5 ± 5.1	10.6 ± 0.0	453	2.49	122
12	0.5	40.4 ± 7.8	4.6 ± 4.6	453	2.05	122
13	1	99 ± 8.4	28.7 ± 10.3	455	1.99	122
14	1	64.3 ± 10.7	17.9 ± 8.4	448	1.69	131
15	0.5−2	39.3 ± 9.4	20.8 ± 9.0	448	1.69	131
16	0.5−1	37.5 ± 11.2	0.0 ± 0.0	448	1.69	131
17	0.5−1	60.7 ± 7.1	27.6 ± 1.3	486	2.66	122
18	1	48.1 ± 12.4	10.1 ± 10.1	448	0.73	142
19	0.5	31.8 ± 8.2	0.0 ± 0.0	419	0.28	134
20	0.5−2	29.1 ± 17.7	13.9 ± 13.9	419	0.28	134
21	1	40.8 ± 14.5	6.7 ± 6.7	419	0.28	134
22	0.5−1	92.3 ± 7.7	18.2 ± 18.2	420	−0.68	147
23	1	100 ± 0.0	21.0 ± 6.0	420	−0.68	147
24	0.5	71.7 ± 2.7	31.7 ± 4.7	420	−0.95	147
25	0.5−1	78.2 ± 21.8	23.3 ± 13.0	408	2.33	146
26	1	87.3 ± 12.7	28.4 ± 0.5	420	−0.11	138
27	1	100 ± 0.0	27.6 ± 1.3	408	0.95	131
28	1	75.4 ± 1.7	22.8 ± 3.5	436	0.95	131
29	1	62.4 ± 14.7	4.2 ± 4.2	436	1.90	131
30	1	87.4 ± 0.6	40.6 ± 8.1	458	2.33	131
31	0.5−1	47.6 ± 5.1	13.2 ± 13.2	424	1.42	122
32	1	100 ± 0.0	21.0 ± 6.0	424	1.42	122
33	0.5−3	93.3 ± 6.7	82.8 ± 11.2	459	2.17	122
34	1	100 ± 0.0	48.7 ± 0.0	503	2.32	122
35	1	53.2 ± 6.8	12.7 ± 2.1	425	0.12	134
36	0.5−3	94.3 ± 5.7	78.1 ± 3.5	526	1.42	122
37	1−2	54.6 ± 5.9	19.1 ± 7.2	382	0.38	122
38	1−2	64.1 ± 10.5	18.3 ± 1.9	424	2.05	122

[a]Effect shown for ipsilateral hind paw; there is no effect on the contralateral side. [b]calculated using ChemBioDraw, version 13.0. [c]ND: not determined.

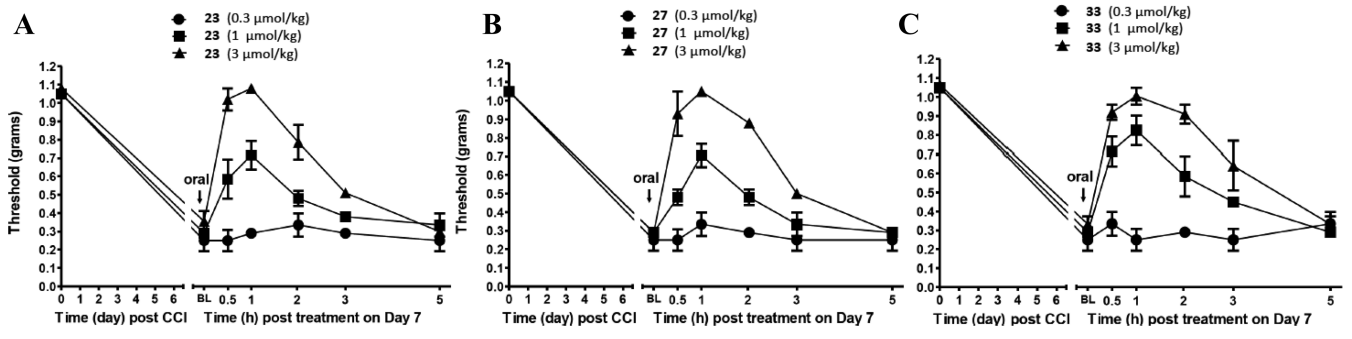

Figure 1. Protection against hind paw allodynia in mice by N^6-methyl derivatives **23**, **27**, and **33** at three doses (po) following CCI of the sciatic nerve. There was no effect on the ipsilateral side (Figure S1, Supporting Information).

expressed in CHO cells, and the $hA_{2A}AR$ was stably expressed in HEK293 cells. The K_i values at the hA_3AR were in most cases in the low nM range. At the hA_1AR and $hA_{2A}AR$, only 10−40% of binding inhibition was seen at 10 μM for all of the tested (N)-methanocarba nucleosides. Thus, there was high hA_3AR selectivity for the entire structural family. The most efficacious

dx.doi.org/10.1021/jm501021n | J. Med. Chem. 2014, 57, 9901−9914

derivatives in the in vivo assay, such as long-acting **33** and **36**, were confirmed to display high selectivity in binding with K_i values at the hA_3AR of 0.70 and 2.68 nM, respectively. However, high A_3AR affinity and selectivity alone were not sufficient to provide full protection in the CCI assay; other analogues that were less efficacious such as *o*-Cl-phenyl derivative **11** were equally A_3AR selective.

Nevertheless, a comparison of AR binding SAR was useful. A comparison of the binding affinities of compounds **6a** and **13** suggests that the presence of an N^6-methyl group in **13** is associated with preserved or increased selectivity for the hA_3AR. Compounds **14**−**16** are regioisomers, in which a methoxy group is moved to different positions on the phenylethynyl ring, but there is little effect on the subnanomolar hA_3AR affinity and selectivity. Compounds **19**−**21** are regioisomers at the pyridylethynyl group, but there is little effect on the hA_3AR affinity. Pyrazine derivatives **22**−**24** similarly display at most a 2-fold difference in hA_3AR binding affinity, and pyrazole derivatives **25** and **26** are similar in hA_3AR affinity. Furyl **27**−**30** and thienyl **31**−**35** derivatives, ferrocene derivative **36**, and cycloalkyl analogues **37** and **38** also displayed only minor variation of nanomolar hA_3AR affinity.

The mAR affinity of selected compounds was measured in binding assays. The mA_3AR affinity of this series of closely related N^6-methyl congeners was typically >30 nM, i.e., reduced > 30-fold in comparison to the hA_3AR affinity. In general, variation of the affinity at mA_3AR was not parallel to changes at the hA_3AR (Figure S1, Supporting Information). The unusual ferrocene derivative **36** was the most potent among these analogues at the mA_3AR with a K_i of 5.46 nM, while many other analogues had K_i values of 30−50 nM. Nevertheless, affinity at the mA_1AR and $mA_{2A}AR$ (single point determination at 10 μM) was very weak, indicating that high A_3AR selectivity (>100-fold for **23**, **27**, **32**, and **33**; >1000-fold for **6a** and **36**) was still present in the mouse.

Selected compounds were examined for functional potency and efficacy at the mA_3AR in an assay of A_3AR-induced inhibition of the production of cyclic AMP in stably transfected HEK293 cells (Figure 2).[22] The tested compounds **23**, **32**, **33**, and **36** were all full agonists at the mA_3AR, with IC_{50} values ranging from 3.14 nM (**36**) to 60.1 nM (**32**). Activity in the inhibition of cyclic AMP formation at the hA_1AR and hA_3AR was evaluated for representative compounds **23** and **32**, which were shown to be potent, full agonists with functional selectivity of roughly 10000-fold for the A_3AR.

Molecular modeling was used to analyze the putative interactions of the distal cyclic groups appended to the *C*2-ethynyl substitutent with the A_3AR. The environment of receptor-bound *C*2-arylethynyl and cycloalkylethynyl groups was explored by docking to A_3AR homology models. We used our previously reported homology models of the h and m A_3ARs,[11,22] based on a hybrid $A_{2A}AR$-β_2 adrenergic receptor template. The hybrid template strategy that determined the outward shift of the extracellular tip of TM2 with the creation of a larger pocket was required to accommodate the rigid and extended *C*2 substituent of these derivatives, as previously described.[11,22] In docking selected compounds of the present series, a common binding mode was obtained at both the h and m A_3AR models, and this mode featured all the key interactions found to anchor the adenine and pseudosugar moieties of similar derivatives. As an example, Figure 3 shows the docking poses of compound **33**, which displayed high affinity at both the hA_3AR (0.70 nM) and mA_3AR (36 nM), at the two receptors. The planar bicyclic core formed a $\pi-\pi$ stacking interaction with a phenylalanine in the second extracellular loop (EL2) and two hydrogen bonds with N6.55, while the methanocarba region formed a hydrogen bonding network with T3.36, S7.42, and H7.43. The *C*2 terminal cyclic group was found to occupy a region close to the extracellular environment in proximity of TM2, with tolerance for many substitutions and steric bulk, consistent with previous findings. Even though the residues in proximity of the terminal cyclic group are different between the h and m A_3ARs, a good accommodation of all the different *C*2 substituents was found in both cases. In the case of compound **33**, the aryl group at the *C*2 position is almost coplanar with the adenine core. However, for other compounds bearing heterocyclic rings with H-bonding donor or acceptor groups, the dihedral angle between the rings can vary to allow formation of H-bonds with residues in EL2, in particular with the backbone NH of Phe168 or with the side chain of Gln167 at the hA_3AR and with the backbone NH of Phe169 or with the side chain of His168 at the mA_3AR.

Interactions with potential off-target receptor sites, which could lead to side effects, were measured for the most promising leads from the in vivo screen. Binding of seven of the most promising N^6-methyl compounds, **23**, **26**, **27**, **32**−**34**, and **36**, to various possible off-target sites (mostly GPCRs) was assayed in a broad screen of binding activity using cloned human or rodent cDNAs for CNS receptors and ion channels. This screening was provided by the National Institute of Mental Health Psychoactive Drug Screening Program (NIMH-PDSP).[26] Data for compounds **1**, **6a**, and **13**, reported elsewhere, are also provided for comparison.[30] Screening results indicated that various analogues displayed significant in vitro binding to other sites in the micromolar range, including biogenic amine receptors. In 44 assays of off-target sites (Supporting Information), compounds **13**, **23**, and **32** at 10 μM inhibited binding by >30% at only a few sites. Various analogues showed significant binding in the μM range at M_2, $5HT_{2A}$, β_3, $5HT_{2B}$, $5HT_{2C}$ (except for diF-phenylethynyl), and α_{2C} receptors and at the translocator protein (TSPO), also known as the peripheral benzodiazepine receptor (PBR). The reference agonist **1** showed interactions (K_i in μM) with $5HT_{2B}$ (1.08) and $5HT_{2C}$ (5.42) receptors. Thus, some of the derivatives have potential off-target activities that could present a liability for drug development. More off-target interaction was observed in the (N)-methanocarba series when an N^6-3-chlorobenzyl group was present, i.e., **6a**;[30] thus, the switch to N^6-methyl was beneficial from this perspective. Compounds **26** and **27** were found to be relatively free of off-target receptor effects in the PDSP screening. Compound **33** was largely free of off-target receptor effects, except at TSPO and σ1 and σ2 receptors. The SAR patterns of the broader chemical series at other GPCRs has been analyzed with the aid of molecular modeling.[30]

In vitro stability measurements in physiological solutions were performed on selected compounds for comparison to the same parameters determined for **6a** to be reported elsewhere (Table 3). Compound **6a** was orally active in vivo in reducing chronic NP, although its physicochemical properties are not optimal (cLogP of 4.15, total polar surface area of 122 Å^2, and molecular weight of 565 D). Thus, it was considered advantageous to find other smaller and less hydrophobic A_3AR agonists that were fully efficacious in vivo against NP. The physicochemical properties of several analogues are predictive of greater drug-like properties in vivo. For example, compound **33** that has a prolonged duration of action displays a more favorable cLogP of 2.17 and molecular weight of 459 D, but the total polar surface area was similar to **6a**. Nevertheless, some compounds clearly in the favored ranges of physicochemical parameters were not among the most

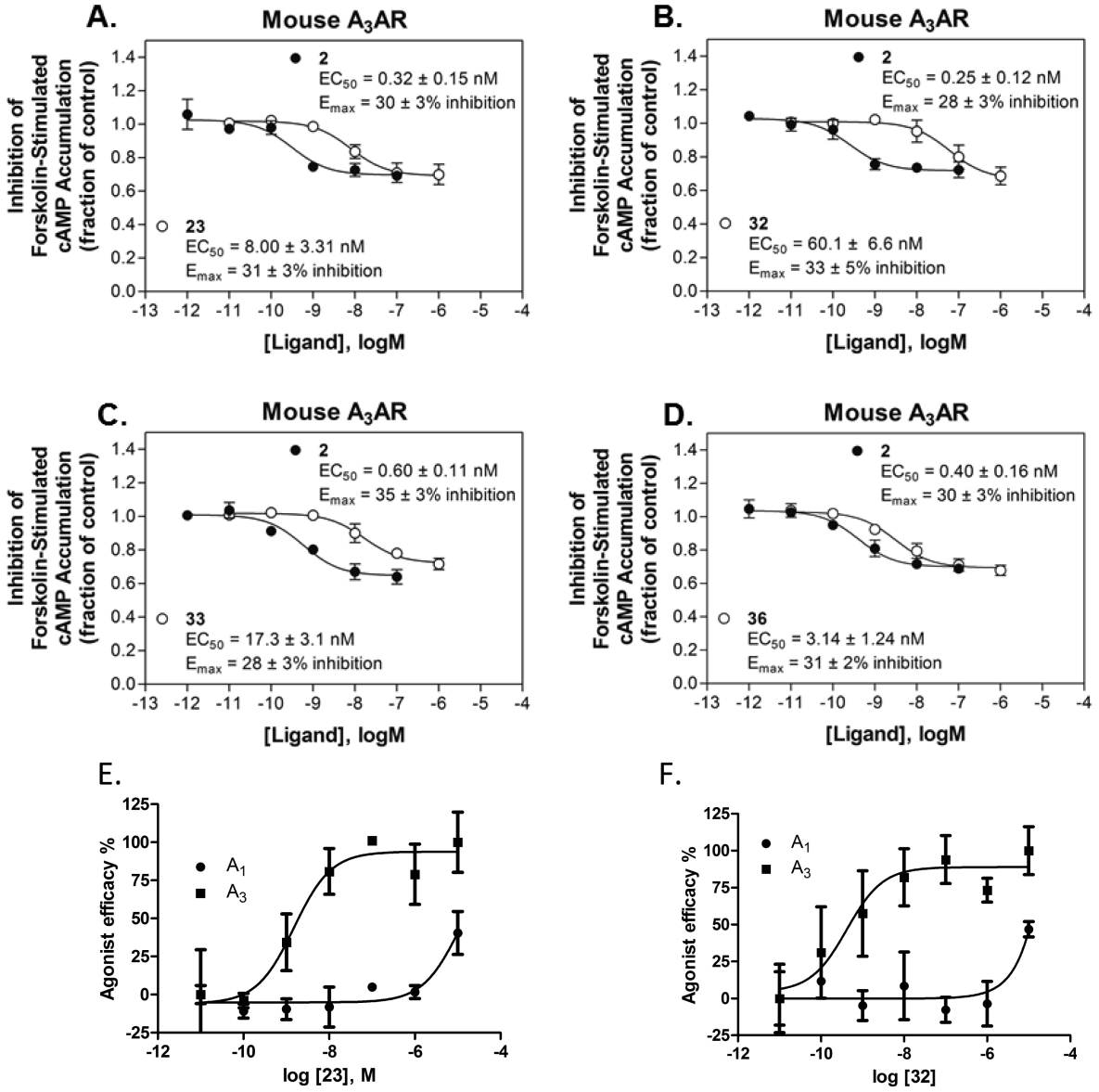

Figure 2. Functional agonism by four selective A_3AR agonists. (A–D) Activity of compounds **23**, **32**, **33**, and **36** in an assay of inhibition of forskolin-stimulated cyclic AMP accumulation with HEK293 cells expressing the mA_3AR.[11,22] Concentration–effect curve with reference full agonist **2** is included for comparison. Data are the mean ± SEM, $n = 4–7$. (E,F) Activity of compounds **23** and **32** in an assay of inhibition of forskolin-stimulated cyclic AMP accumulation with CHO cells expressing the hA_3AR.[11] EC_{50} values are **23**, 1.46 ± 0.37 nM; **32**, 0.42 ± 0.18 nM.

efficacious in vivo. Thus, the in vivo effects are not ascribable to a simple combination of parameters. The solubility of pyrazinyl **23** and furyl **27** derivatives was greatly increased (>0.2 mg/mL) and plasma protein binding in three species diminished (24–61% free) while the in vivo efficacy of this analogue was maintained.

Stability tests (Table 3) indicated that **23**, **27**, **33**, and **34** are stable in liver microsomes of three species (human, rat, and mouse) and in simulated body fluids (gastric, intestinal), but **36** is rapidly degraded ($t_{1/2}$ in microsomes = 2–7 min). Therefore, it is likely that the long-lasting protective effects of **36** in the phenotypic screen are from an unidentified metabolite that forms in vivo. There was an unfavorable CYP450 inhibition profile for bromothienyl derivative **34**, with a measurable IC_{50} value of 7.4 μM for the 2D6 isozyme. Compound **34** inhibited the 3A4 isozyme with an IC_{50} value of 9.4 μM. Compounds **23**, **27**, and **33** were shown not to be substrates for P-glycoprotein in a study of bidirectional permeability in a CACO-2 cell monolayer (Supporting Information). **27** and **33** displayed moderate apical to basal permeability, and **23** displayed low permeability. Selected compounds were examined by the PDSP for functional inhibition of hERG K^+ channels (% inhibition at 10 μM or IC_{50}): **6a** (12.2 μM), **13** (27 μM), **26** (28%), **27** (21%), **32** (11.5 μM), and **33** (12.9 μM). Thus, the hA_3AR binding affinity of these analogues exceeds hERG inhibition by typically 10,000-fold.

DISCUSSION

Phenotypic screening is making a resurgence as a strategy in drug discovery.[31] Although our approach is target-based at the outset, i.e., we have narrowed the structural scope based on new compounds consistent with a well developed SAR at the A_3AR, we have subjected the next stage of refinement to an in vivo screen that combines multiple components of pharmacokinetics and possible interaction with multiple mechanisms as well as the main mechanism of AR activation. We have administered the

dx.doi.org/10.1021/jm501021n | J. Med. Chem. 2014, 57, 9901–9914

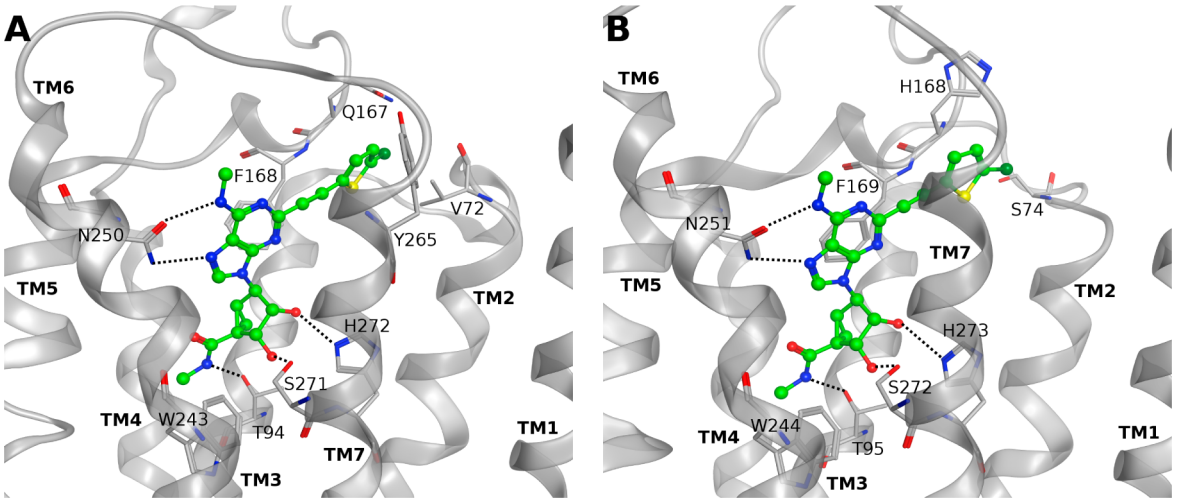

Figure 3. Putative binding modes of 2-(2-chlorothienylethynyl)-N^6-methyl (N)-methanocarba derivative **33** (green carbons) obtained after docking simulations: (A) at the hA_3AR, (B) at the mA_3AR. Side chains of some amino acids important for ligand recognition are highlighted. H-Bonds are pictured as dotted lines. Hydrogen atoms are not displayed. The corresponding residue numbers of the hA_3AR using the Ballesteros–Weinstein notation[46] or locations are V72, 2.64; T94, 3.36; Q167, EL2; F168, EL2; W243, 6.48; N250, 6.55; Y265, 7.36; S271, 7.42; H272, 7.43.

Table 3. In Vitro Stability Parameters for Selected Nucleoside Derivatives

	compound				
test	**23**	**27**	**33**	**34**	**36**
aq solubility (pH 7.4, μg/mL)[a]	>208	>202	16.8 ± 1.1	15.6 ± 0.9	14.5 ± 1.0
stability in simulated fluids ($t_{1/2}$, min)					
gastric (pH 1.6)	>480	>480	>480	>480	46.5
intestinal (pH 6.5)	>480	>480	>480	>480	174
% unbound in plasma					
human	61.2	24.2	6.22	2.67	7.00
rat	57.5	40.5	5.91	4.04	6.32
mouse	59.1	50.2	6.40	2.75	4.85
inhibition of 5 CYP isozymes (IC_{50}, μM)	>10	>10	>10	>7[b]	>9[c]
stability in liver microsomes ($t_{1/2}$, min)					
human[d]	236	145	230	205	3.66
rat	>145	140	128	91	6.64
mouse	>145	141	143	96	1.98

[a]mean (±SD, where given) for n = 3. [b]% inhibition at 10 μM **34**: 1A2, 15.0; 2C9, 24.2; 2C19, 34.0; 2D6, 57.5 (IC_{50} 7.4 μM); 3A4, 3.1 (average of n = 2). [c]% inhibition at 10 μM **36**: 1A2, 30.5; 2C9, 17.2; 2C19, 18.1; 2D6, 20.5; 3A4, 51.6 (IC_{50} 9.4 μM), (average of n = 2). [d]CL_{int} values (μL/min/mg protein) in human liver microsomes: **23**, 2.99; **27**, 3.09; **33**, 3.69; **34**, 3.38.

nucleosides orally, which is the preferred route for a chronic pain drug.

We have recently reported that A_3AR agonists including **6a** are more potent than currently used analgesics (gabapentin, amitriptyline, morphine);[10] in contrast to opioids, these do not cause tolerance upon repeated administration and are not rewarding.[6,10] The mechanisms of action whereby A_3AR agonists block and reverse neuropathic pain states do not rely upon an endogenous opioid or endocannabinoid pathway[6,10] but do rely upon activation of A_3AR found in spinal cord dorsal horn and at supraspinal sites (i.e., in the RVM) to engage descending inhibitory noradrenergic and serotonergic bulbospinal systems, leading to reduced spinal neuronal hyperexcitability.[6] It is noteworthy that A_3AR attenuates neuropathic pain at least in part by reducing neuro-glia dysfunction and downstream neuroinflammatory events that are critical to the development of neuronal excitability associated with central sensitization, inhibition of spinal glial cell activation and redox-sensitive signaling transduction pathways (MAPK kinases and NFκB) leading to overall reduction in proinflammatory cytokines (TNF and IL1β but increased levels of the potent anti-inflammatory and neuroprotective cytokine, IL-10).[15,16] The discovery of highly selective A_3AR agonist such as those described in this paper provides a necessary pharmacological tool to enable our mechanistic understanding of the roles of the A_3AR in chronic pain states and therefore the impact of targeting this receptor to alleviate chronic pain and human suffering, thus addressing a huge medical need with major socioeconomic consequences.

The in vivo activities of various N^6-methyl derivatives were compared and correlated with structure, and several preferred candidates have been identified. The unsubstituted *C*2-phenylethynyl analogue **7a** displayed low efficacy (44% of full reversal at peak effect) in the CCI model of chronic NP. The extended biphenyl derivative **7b** also displayed less than full efficacy. Aryl halogenation is a possible approach to lengthening the in vivo duration of action by preventing oxidation by cytochrome P450 enzymes in the liver.[32] However, the monohalophenylethynyl analogues **8**–**12** were less than fully efficacious, and the

dx.doi.org/10.1021/jm501021n | J. Med. Chem. 2014, 57, 9901–9914

3,4-difluorophenyl group of the more efficacious **13** resulted in a shorter peak duration in comparison to reference compound **6a**. Substitution of the phenyl ring with methoxy improved the maximal effect (64%) but only in the ortho position in **14**. All positions of nitrogen in the pyridyl analogues **19**, **20**, and **21** resulted in the same or lower efficacy than the phenyl analogue **7a**. However, dinitrogen substitution in pyrazine derivative **23** increased the efficacy to ∼100%, but the efficacy of isomers containing nitrogen at different positions in **22** and **24** resulted in less than full efficacy. A pyrazine moiety is found in many natural products and drug-like molecules such as the diuretic amiloride.[33] 2-Furyl **27** and 2-thienyl **32** analogues were fully efficacious, with a ∼3 h duration of action. Curiously, duration and efficacy of a 3-thienyl analogue **31** was considerably lower. Addition of 5-chloro to the 2-thienyl analogue **32**, resulting in compound **33**, prolonged the duration of action while maintaining full efficacy, and 5-bromothienyl substitution in **34** was also well tolerated in vivo and in binding (K_i 0.4 nM). A similar 5-chlorothiophene-2-carboxamide moiety was found to be relatively metabolically stable in a widely used anticoagulant Rivaroxaban.[34]

The ferrocene derivative **36** was fully efficacious, but the toxicological properties of this organometallic compound were not tested. Other ferrocene compounds, such as anticancer derivatives of tamoxifen, were found to be biocompatible and not highly toxic.[35] Thus, **36** was considered to be a candidate for further biological evaluation. A class of organometallic (ruthenium) heterocyclic derivatives has already been reported as A_3AR antagonists.[36] Cycloalkyl analogues **37** and **38** displayed less than full efficacy in vivo (60−70%). Among mono- and dihalo-substituted analogues, the 3,4-difluoro analogue **13**, bearing the same *C*2 substituent as reference compound **6a**, was the most efficacious.

Thus, the effects of introducing a 2-alkynyl group in adenosine (riboside) derivatives on their AR affinity and selectivity have been variable.[37] In some cases, selectivity for the A_3AR has been achieved. In the present series of nucleoside derivatives that contain several sources of conformational rigidity, the nM affinity and nearly complete specificity for the A_3AR is maintained for a wide variety of cyclic groups attached to the 2-ethynyl moiety. Docking studies confirmed that the A_3AR has sufficient plasticity in the region around the extracellular tip of TM2 to accommodate a wide range of steric and electronic character, allowing the rest of the ligand molecule to strongly interact with all the key residues important for AR binding. Thus, we have extended previous 2-phenylethynyl series[22] to provide a great breadth of substitution that preserves target specificity. In summary, the analogues that reached nearly full efficacy in reversing NP in vivo were **13**, **22**, **23**, **26**, **27**, **32**, **33**, **34**, and **36**. Thus, both 2-thienyl and 2-furyl derivatives are among the most efficacious analogues in vivo.

One of the major reasons for failure of a variety of AR ligands on a clinical path was low bioavailabily.[19] Therefore, there was a need to optimize physicochemical characteristics that are predictive of bioavailability. The smaller molecular weight and lower hydrophobicity of the N^6-methyl analogues in comparison to the reference A_3AR agonist **6a** are consistent with drug-like properties in vivo. Compound **6a** suffers from high hydrophobicity, leading to low aqueous solubility. Pyrazine derivative **23** is much more polar than **6a** and consequently more water-soluble and less bound to plasma proteins, and it displays good efficacy in the CCI model. Furan **27** and 2-chlorothiophene **33** derivatives are fully efficacious in CCI model and display a 5-fold higher hA_3AR affinity than **6a**. Compound **33** had a favorable combination of physicochemical parameters within this group of nucleosides. Moreover, compound **27** completely lacks off-target interactions at 10 μM and has a relatively low molecular weight (408), predictive of increased bioavailability, and possibly CNS entry. Thus, we have expanded the structural range of orally active adenosine derivatives for the treatment of chronic pain. The most efficacious compounds in vivo had a cLogP of ≤2.3 and a tPSA of ≤131 Å^2. However, there appears to be no direct correlation between the in vivo efficacy against NP and the three physicochemical parameters listed in Table 3. A molecular weight of 526 in potentially short-lived ferrocene derivative **36** still allowed full efficacy, as did a tPSA of >120 (e.g., **23**), which is considered the upper limit for molecules expected to readily cross the blood brain barrier.[23]

Three 2-thienyl derivatives were among the most efficacious and long lasting in vivo. The in vivo metabolism of thiophene derivatives has been studied.[38] Cytochrome P450s may catalyze the oxidation of thiophene compounds with the simultaneous formation of two reactive intermediates, a thiophene-*S*-oxide and a thiophene epoxide. However, some 5-halothiophene derivatives demonstrate greater stability in vivo.[34] Strikingly, in this study, the in vivo pharmacological effects of 5-substituted thiophene derivatives **33** and **34** were among the most prolonged. These compounds were sufficiently stable in vivo to provide an extended duration of action compared to the majority of other analogues, suggesting that rapid degradation is not occurring in these derivatives. Both compounds were stable in liver microsomes, but compound **34** inhibited a CYP450 isozyme in the μM range; therefore, **33** appears to be the leading candidate molecule arising from this study.

■ CONCLUSIONS

The translation of AR agonists into therapeutic products has been impeded by efficacy, bioavailability, and side effect issues.[19] This study progresses beyond the most common initial screen of binding selectivity alone to some of parameters that are predictive of derisking in pharmaceutical development such as oral bioactivity.

We have modified the *C*2-arylethynyl group of our previously reported A_3AR agonists with different rings, including both substituted benzene rings and small heterocyclic rings like thiophene. These are mostly in the N^6-methyl series, which has reduced affinity at the mouse A_3AR but may be advantageous because of favorable pharmacokinetics over the N^6-benzyl series due to a lower MW and lower log *P*. Five-membered heteroring derivatives **27** and **32**−**34** were fully efficacious in reducing neuropathic pain in vivo, suggesting structural consistency. An unusual organometallic derivative **36** was among those compounds showing a prolonged duration of action that would not have been predicted from the binding affinity alone, but this compound was unstable under physiological conditions. The most promising fully efficacious analogues in this study, with respect to aqueous solubility and absence of off-target sites, were pyrazinyl **23** and furyl **27** derivatives. 5-Chlorothienyl derivative **33** had a favorable balance of high and prolonged efficacy, predicted in vivo stability, and few off-target interactions. Measuring the potential off-target effects, such as interaction with α-adrenergic receptors, provides another means of identifying possible liabilities early in the drug discovery process. The lead compounds discovered here are now suitable for more extensive in vivo testing, including pharmacokinetic and toxicity evaluation. On the basis of these leads, we hope to identify other highly efficacious analogues with in vivo activity using phenotypic screening.

dx.doi.org/10.1021/jm501021n | J. Med. Chem. 2014, 57, 9901−9914

EXPERIMENTAL SECTION

Chemical Synthesis. *Materials and Instrumentation.* All reagents and solvents were purchased from Sigma-Aldrich (St. Louis, MO). ^{1}H NMR spectra were obtained with a Bruker 400 spectrometer using $CDCl_3$ and CD_3OD as solvents. Chemical shifts are expressed in δ values (ppm) with tetramethylsilane (δ 0.00) for $CDCl_3$ and water (δ 3.30) for CD_3OD. TLC analysis was carried out on glass sheets precoated with silica gel F254 (0.2 mm) from Aldrich. All the final sulfonate nucleoside compounds were purified by HPLC with a Luna 5 μmRP-C18(2) semipreparative column (250 mm × 10.0 mm; Phenomenex, Torrance, CA) and using the following conditions: flow rate of 2 mL/min, 10 mM trifluoroacetic acid−water (TFA−H_2O)−CH_3CN from 80:20 to 30:70 in 20−40 min. The purity of final nucleoside derivatives was checked using a Hewlett−Packard 1100 HPLC equipped with a Zorbax SB-Aq 5 μm analytical column (50 mm × 4.6 mm; Agilent Technologies Inc., Palo Alto, CA). Mobile phase: linear gradient solvent system, 5 mM TBAP (tetrabutylammonium dihydrogen phosphate)−CH_3CN from 80:20 to 0:100 in 13 min; the flow rate was 0.5 mL/min. Peaks were detected by UV absorption with a diode array detector at 230, 254, and 280 nm. All derivatives tested for biological activity showed >95% purity by HPLC analysis (detection at 254 nm). Low-resolution mass spectrometry was performed with a JEOL SX102 spectrometer with 6 kV Xe atoms, following desorption from a glycerol matrix or on an Agilent LC/MS 1100 MSD with a Waters (Milford, MA) Atlantis C18 column. High resolution mass spectroscopic (HRMS) measurements were performed on a proteomics optimized Q-TOF-2 (Micromass-Waters) using external calibration with polyalanine, unless noted. Observed mass accuracies are those expected based on known performance of the instrument as well as trends in masses of standard compounds observed at intervals during the series of measurements. Reported masses are observed masses uncorrected for this time-dependent drift in mass accuracy. Compound **40** was prepared as reported.[22] All of the monosubsituted alkyne intermediates were purchased from Sigma-Aldrich (St. Louis, MO), Small Molecules, Inc. (Hoboken, NJ), Anichem (North Brunswick, NJ), PharmaBlock, Inc. (Sunnyvale, CA), Frontier Scientific (Logan, UT), and Tractus (Perrineville, NJ).

*(1S,2R,3S,4R,5S)-2,3-Dihydroxy-4-(2-((2-methoxyphenyl)ethynyl)-6-(methylamino)-9H-purin-9-yl)-N-methylbicyclo[3.1.0]hexane-1-carboxamide (**14**).* Compound **14** (69%) was prepared from compound **40** following the same method for compound **22**. ^{1}H NMR (CD_3OD, 600 MHz) δ 8.10 (s, 1H), 7.59 (d, J = 6.0 Hz, 1H), 7.45 (t, J = 7.2 Hz, 1H), 7.10 (d, J = 8.4 Hz, 1H), 7.01 (t, J = 7.2 Hz, 1H), 5.15 (d, J = 6.0 Hz, 1H), 4.90 (s, 1H), 4.04 (d, J = 6.0 Hz, 1H), 3.96 (s, 3H), 3.15 (br s, 3H), 2.82 (s, 3H), 2.09−2.07 (m, 1H), 1.86 (t, J = 4.8 Hz, 1H), 1.43−1.41 (m, 1H). HRMS calculated for $C_{23}H_{25}N_6O_4$ $(M + H)^+$, 449.1937; found, 449.1932.

*(1S,2R,3S,4R,5S)-2,3-Dihydroxy-4-(2-((3-methoxyphenyl)ethynyl)-6-(methylamino)-9H-purin-9-yl)-N-methylbicyclo[3.1.0]hexane-1-carboxamide (**15**).* Compound **15** (69%) was prepared from compound **40** following the same method for compound **22**. ^{1}H NMR (CD_3OD, 400 MHz) δ 8.10 (s, 1H), 7.35 (t, J = 6.0 Hz, 1H), 7.24−7.21 (m, 2H), 7.02 (d, J = 8.4 Hz, 1H), 5.06 (d, J = 6.8 Hz, 1H), 4.92 (s, 1H), 4.02 (d, J = 6.4 Hz, 1H), 3.85 (s, 3H), 3.15 (br s, 3H), 2.84 (s, 3H), 2.13−2.09 (m, 1H), 1.88 (t, J = 4.4 Hz, 1H), 1.41−1.38 (m, 1H). HRMS calculated for $C_{23}H_{25}N_6O_4$ $(M + H)^+$, 449.1937; found, 449.1944.

*(1S,2R,3S,4R,5S)-2,3-Dihydroxy-4-(2-((4-methoxyphenyl)ethynyl)-6-(methylamino)-9H-purin-9-yl)-N-methylbicyclo[3.1.0]hexane-1-carboxamide (**16**).* Compound **16** (68%) was prepared from compound **40** following the same method for compound **22**. ^{1}H NMR (CD_3OD, 400 MHz) δ 8.08 (s, 1H), 7.60 (d, J = 9.2 Hz, 1H), 7.01 (d, J = 9.2 Hz, 1H), 5.05 (d, J = 5.2 Hz, 1H), 4.91 (s, 1H), 4.02 (d, J = 6.0 Hz, 1H), 3.86 (s, 3H), 3.15 (br s, 3H), 2.85 (s, 3H), 2.13−2.09 (m, 1H), 1.88 (t, J = 5.2 Hz, 1H), 1.41−1.39 (m, 1H). HRMS calculated for $C_{23}H_{25}N_6O_4$ $(M + H)^+$, 449.1937; found, 449.1944.

*(1S,2S,3R,4R,5S)-2,3-Dihydroxy-N-methyl-4-(6-(methylamino)-2-((3-(trifluoromethyl)phenyl)ethynyl)-9H-purin-9-yl)bicyclo[3.1.0]hexane-1-carboxamide (**17**).* Compound **17** (70%) was prepared from compound **40** following the same method for compound **22**. ^{1}H NMR (CD_3OD, 400 MHz) δ 8.14 (s, 1H), 7.97 (s, 1H), 7.92 (d, J = 7.6 Hz, 1H), 7.78 (d, J = 7.6 Hz, 1H), 7.68 (t, J = 8.0 Hz, 1H), 5.08 (d, J = 4.8 Hz, 1H), 4.90 (s, 1H), 4.04 (d, J = 5.2 Hz, 1H), 3.15 (br s, 3H), 2.84 (s, 3H), 2.13−2.10 (m, 1H), 1.88 (t, J = 5.2 Hz, 1H), 1.42−1.39 (m, 1H). HRMS calculated for $C_{23}H_{22}N_6O_3F_3$ $(M + H)^+$, 487.1705; found, 487.1716.

*(1S,2R,3S,4R,5S)-2,3-Dihydroxy-4-(2-((4-(hydroxymethyl)phenyl)-ethynyl)-6-(methylamino)-9H-purin-9-yl)-N-methylbicyclo[3.1.0]-hexane-1-carboxamide (**18**).* Compound **18** (66%) was prepared from compound **40** following the same method for compound **22**. ^{1}H NMR (CD_3OD, 400 MHz) δ 8.13 (s, 1H), 7.63 (d, J = 8.0 Hz, 2H), 7.43 (d, J = 8.0 Hz, 2H), 5.06 (d, J = 6.4 Hz, 1H), 4.89 (s, 1H), 4.67 (s, 2H), 4.02 (d, J = 6.4 Hz, 1H), 3.15 (br s, 3H), 2.84 (s, 3H), 2.13−2.09 (m, 1H), 1.88 (d, J = 4.8 Hz, 1H), 1.41−1.39 (m, 1H). HRMS calculated for $C_{23}H_{25}N_6O_4$ $(M + H)^+$, 449.1937; found, 449.1942.

*(1S,2R,3S,4R,5S)-2,3-Dihydroxy-N-methyl-4-(6-(methylamino)-2-(pyridin-3-ylethynyl)-9H-purin-9-yl)bicyclo[3.1.0]hexane-1-carboxamide (**20**).* Compound **20** (60%) was prepared from compound **40** following the same method for compound **22**. ^{1}H NMR (CD_3OD, 400 MHz) δ 8.87 (s, 1H), 8.64 (s, 1H), 8.18 (d, J = 6.4 Hz, 1H), 8.15 (s, 1H), 7.61−7.58 (m, 1H), 5.05 (d, J = 5.2 Hz, 1H), 4.90 (s, 1H), 4.02 (d, J = 5.2 Hz, 1H), 3.13 (br s, 3H), 2.82 (s, 3H), 2.11−2.09 (m, 1H), 1.87 (t, J = 4.0 Hz, 1H), 1.40−1.37 (m, 1H). HRMS calculated for $C_{21}H_{22}N_7O_3$ $(M + H)^+$, 420.1784; found, 420.1785.

*(1S,2R,3S,4R,5S)-2,3-Dihydroxy-N-methyl-4-(6-(methylamino)-2-(pyridin-4-ylethynyl)-9H-purin-9-yl)bicyclo[3.1.0]hexane-1-carboxamide (**21**).* Compound **21** (63%) was prepared from compound **40** following the same method for compound **22**. ^{1}H NMR (CD_3OD, 400 MHz) δ 8.63 (d, J = 6.0 Hz, 2H), 8.14 (s, 1H), 7.65 (d, J = 6.0 Hz, 1H), 5.06 (d, J = 6.0 Hz, 1H), 4.90 (s, 1H), 4.03 (d, J = 6.8 Hz, 1H), 3.14 (br s, 3H), 2.13−2.10 (m, 1H), 1.88 (d, J = 4.8 Hz, 1H), 1.42−1.40 (m, 1H). HRMS calculated for $C_{21}H_{22}N_7O_3$ $(M + H)^+$, 420.1784; found, 420.1786.

*(1S,2R,3S,4R,5S)-2,3-Dihydroxy-N-methyl-4-(6-(methylamino)-2-(pyrimidin-2-ylethynyl)-9H-purin-9-yl)bicyclo[3.1.0]hexane-1-carboxamide (**22**).* $PdCl_2(PPh_3)_2$ (6.08 mg, 0.02 mmol), CuI (1.0 mg, 0.005 mmol), 2-ethynylpyrimidine (27.1 mg, 0.26 mmol), and triethylamine (0.06 mL, 0.43 mmol) were added to a solution of compound **40** (21 mg, 0.04 mmol) in anhydrous DMF (1 mL), and the mixture stirred at room temperature overnight. Solvent was evaporated under vacuum, and the residue was roughly purified on flash silica gel column chromatography. The resulting compound was dissolved in MeOH (2 mL) and 10% trifluoroacetic acid (2 mL) and heated at 70 °C for 5 h. Solvent was evaporated under vacuum, and the residue was purified on flash silica gel column chromatography (CH_2Cl_2:MeOH = 25:1) to give the compound **22** (12.2 mg, 67%) as syrup. ^{1}H NMR (CD_3OD, 400 MHz) δ 8.86 (d, J = 5.2 Hz, 2H), 8.14 (s, 1H), 7.53 (t, J = 5.2 Hz, 1H), 5.17 (d, J = 6.8 Hz, 1H), 4.92 (s, 1H), 4.6 (d, J = 6.4 Hz, 1H), 3.14 (br s, 3H), 2.86 (s, 3H), 2.11−2.07 (m, 1H), 1.84 (t, J = 5.2 Hz, 1H), 1.42−1.39 (m, 1H). HRMS calculated for $C_{20}H_{21}N_8O_3$ $(M + H)^+$, 421.1737; found, 421.1732.

*(1S,2R,3S,4R,5S)-2,3-Dihydroxy-N-methyl-4-(6-(methylamino)-2-(pyrazin-2-ylethynyl)-9H-purin-9-yl)bicyclo[3.1.0]hexane-1-carboxamide (**23**).* Compound **23** (65%) was prepared from compound **40** following the same method for compound **22**. ^{1}H NMR (CD_3OD, 400 MHz) δ 8.92 (s, 1H), 8.69 (d, J = 2.4 Hz, 1H), 8.64 (d, J = 2.4 Hz, 1H), 8.14 (s, 1H), 5.12 (d, J = 5.2 Hz, 1H), 4.89 (s, 1H), 4.05 (d, J = 6.4 Hz, 1H), 3.15 (br s, 3H), 2.85 (s, 3H), 2.12−2.08 (m, 1H), 1.86 (t, J = 5.2 Hz, 1H), 1.42−1.40 (m, 1H). HRMS calculated for $C_{20}H_{21}N_8O_3$ $(M + H)^+$, 421.1737; found, 421.1725.

*(1S,2R,3S,4R,5S)-2,3-Dihydroxy-N-methyl-4-(6-(methylamino)-2-(pyridazin-3-ylethynyl)-9H-purin-9-yl)bicyclo[3.1.0]hexane-1-carboxamide (**24**).* Compound **24** (65%) was prepared from compound **40** following the same method for compound **22**. ^{1}H NMR (CD_3OD, 400 MHz) δ 9.23 (d, J = 3.2 Hz, 1H), 8.15 (s, 1H), 8.03 (d, J = 6.8 Hz, 1H), 7.83−7.81 (m, 1H), 5.14 (d, J = 5.2 Hz, 1H), 4.90 (s, 1H), 4.07 (d, J = 5.2 Hz, 1H), 3.15 (br s, 3H), 2.84 (s, 3H), 2.11−2.08 (m, 1H), 1.86 (t, J = 4.8 Hz, 1H), 1.42−1.39 (m, 1H). HRMS calculated for $C_{20}H_{21}N_8O_3$ $(M + H)^+$, 421.1737; found, 421.1734.

*(1S,2R,3S,4R,5S)-4-(2-((1H-Pyrazol-3-yl)ethynyl)-6-(methylamino)-9H-purin-9-yl)-2,3-dihydroxy-N-methylbicyclo[3.1.0]hexane-1-carboxamide (**25**).* Compound **25** (64%) was prepared from compound **40** following the same method for compound **22**. ^{1}H NMR (CD_3OD, 400 MHz) δ 8.10 (s, 1H), 7.73 (s, 1H), 6.66 (s, 1H), 5.12 (d, J = 6.8 Hz,

dx.doi.org/10.1021/jm501021n | J. Med. Chem. 2014, 57, 9901−9914

1H), 4.87 (s, 1H), 4.04 (d, J = 6.8 Hz, 1H), 3.13 (br s, 3H), 2.85 (s, 3H), 2.10−2.07 (m, 1H), 1.85 (t, J = 4.8 Hz, 1H), 1.41−1.38 (m, 1H). HRMS calculated for $C_{19}H_{21}N_8O_3$ $(M + H)^+$, 409.1737; found, 409.1731.

*(1S,2R,3S,4R,5S)-2,3-Dihydroxy-N-methyl-4-(2-((1-methyl-1H-pyrazol-4-yl)ethynyl)-6-(methylamino)-9H-purin-9-yl)bicyclo[3.1.0]hexane-1-carboxamide (**26**).* Compound **26** (63%) was prepared from compound **40** following the same method for compound **22**. ^{1}H NMR (CD_3OD, 400 MHz) δ 8.08 (s, 1H), 7.98 (s, 1H), 7.75 (s, 1H), 5.05 (d, J = 5.6 Hz, 1H), 4.88 (s, 1H), 4.02 (d, J = 6.4 Hz, 1H), 3.94 (s, 3H), 3.13 (br s, 3H), 2.86 (d, J = 4.4 Hz, 1H), 2.12−2.08 (m, 1H), 1.87 (t, J = 4.8 Hz, 1H), 1.41−1.37 (m, 1H). HRMS calculated for $C_{20}H_{23}N_8O_3$ $(M + H)^+$, 423.1888; found, 423.1888.

*(1S,2R,3S,4R,5S)-4-(2-(Furan-2-ylethynyl)-6-(methylamino)-9H-purin-9-yl)-2,3-dihydroxy-N-methylbicyclo[3.1.0]hexane-1-carboxamide (**27**).* Compound **27** (58%) was prepared from compound **40** following the same method for compound **22**. ^{1}H NMR (CD_3OD, 400 MHz) δ 8.16 (s, 1H), 7.66 (d, J = 1.2 Hz, 1H), 6.95 (d, J = 2.8 Hz, 1H), 6.58 (dd, J_1 =1.6, J_2 = 2.0 Hz, 1H), 5.07 (d, J = 5.2 Hz, 1H), 4.89 (s, 1H), 4.03 (d, J = 6.4 Hz, 1H), 3.14 (br s, 3H) 2.87 (s, 3H), 2.11−2.09 (m, 1H), 1.86 (t, J = 4.8 Hz, 1H), 1.41−1.40 (m, 1H). HRMS calculated for $C_{20}H_{21}N_6O_4$ $(M + H)^+$, 409.1624; found, 409.1611.

*(1S,2R,3S,4R,5S)-4-(2-((4,5-Dimethylfuran-2-yl)ethynyl)-6-(methylamino)-9H-purin-9-yl)-2,3-dihydroxy-N-methylbicyclo[3.1.0]hexane-1-carboxamide (**28**).* Compound **28** (63%) was prepared from compound **40** following the same method for compound **35**. ^{1}H NMR (CD_3OD, 400 MHz) δ 8.09 (s, 1H), 6.69 (s, 1H), 5.06 (d, J = 6.4 Hz, 1H), 4.85 (s, 1H), 4.01 (d, J = 6.4 Hz, 1H), 3.12 (br s, 3H), 2.87 (s, 3H), 2.26 (s, 3H), 2.12−2.08 (m, 1H), 1.99 (s, 3H), 1.85 (t, J = 4.8 Hz, 1H), 1.40−1.38 (m, 1H). HRMS calculated for $C_{22}H_{25}N_6O_4$ $(M + H)^+$, 437.1932; found, 437.1934.

*(1S,2R,3S,4R,5S)-4-(2-((5-Ethylfuran-2-yl)ethynyl)-6-(methylamino)-9H-purin-9-yl)-2,3-dihydroxy-N-methylbicyclo[3.1.0]hexane-1-carboxamide (**29**).* Compound **29** (53%) was prepared from compound **40** following the same method for compound **22**. ^{1}H NMR (CD_3OD, 400 MHz) δ 8.11 (s, 1H), 6.82 (d, J = 7.2 Hz, 1H), 6.18 (d, J = 7.6 Hz, 1H), 5.08 (d, J = 6.4 Hz, 1H), 4.93 (s, 1H), 4.02 (d, J = 6.4 Hz, 1H), 3.14 (br s, 3H), 2.75−2.69 (m, 2H), 2.11−2.08 (m, 1H), 1.86 (t, J = 5.2 Hz, 1H), 1.41−1.38 (m, 1H), 1.29 (t, J = 7.6 Hz, 3H). HRMS calculated for $C_{22}H_{25}N_6O_4$ $(M + H)^+$, 437.1932; found, 437.1932.

*(1S,2R,3S,4R,5S)-4-(2-(Benzofuran-2-ylethynyl)-6-(methylamino)-9H-purin-9-yl)-2,3-dihydroxy-N-methylbicyclo[3.1.0]hexane-1-carboxamide (**30**).* Compound **30** (62%) was prepared from compound **40** following the same method for compound **22**. ^{1}H NMR (CD_3OD, 400 MHz) δ 8.12 (s, 1H), 7.67 (d, J = 7.6 Hz, 1H), 7.5 (d, J = 7.6 Hz, 1H), 7.43 (t, J = 6.0 Hz, 1H), 7.33−7.31 (m, 2H), 5.11 (d, J = 5.2 Hz, 1H), 4.89 (s, 1H), 4.04 (d, J = 6.4 Hz, 1H), 3.15 (br s, 3H), 2.89 (s, 3H), 2.13−2.10 (m, 1H), 1.87 (t, J = 4.8 Hz, 1H), 1.42−1.39 (m, 1H). HRMS calculated for $C_{24}H_{23}N_6O_4$ $(M + H)^+$, 459.1775; found, 459.1777.

*(1S,2R,3S,4R,5S)-2,3-Dihydroxy-N-methyl-4-(6-(methylamino)-2-(thiophen-3-ylethynyl)-9H-purin-9-yl)bicyclo[3.1.0]hexane-1-carboxamide (**31**).* Compound **31** (59%) was prepared from compound **40** following the same method for compound **22**. ^{1}H NMR (CD_3OD, 400 MHz) δ 8.13 (s, 1H), 7.88 (dd, J_1 = 1.2, J_2 = 2.0 Hz, 1H), 7.54 (dd, J_1 = 2.0, J_2 = 3.2 Hz, 1H), 7.33 (dd, J_1 = 1.2, J_2 = 4.0 Hz, 1H), 5.07 (d, J = 5.2 Hz, 1H), 4.89 (s, 1H), 4.04 (d, J = 5.2 Hz, 1H), 3.15 (br s, 3H), 2.85 (s, 3H), 2.13−2.09 (m, 1H), 1.87 (t, J = 4.8 Hz, 1H), 1.42−1.39 (m, 1H). HRMS calculated for $C_{20}H_{21}N_6O_3S$ $(M + H)^+$, 425.1396; found, 425.1403.

*(1S,2R,3S,4R,5S)-2,3-Dihydroxy-N-methyl-4-(6-(methylamino)-2-(thiophen-2-ylethynyl)-9H-purin-9-yl)bicyclo[3.1.0]hexane-1-carboxamide (**32**).* Compound **32** (61%) was prepared from compound **40** following the same method for compound **22**. ^{1}H NMR (CD_3OD, 400 MHz) δ 8.10 (s, 1H), 7.57 (dd, J_1 = 1.2, J_2 = 4.0 Hz, 1H), 7.50 (dd, J_1 = 1.2, J_2 = 4.0 Hz, 1H), 7.13 (dd, J_1 = 1.6, J_2 = 3.6 Hz, 1H), 5.05 (d, J = 6.4 Hz, 1H), 4.88 (s, 1H), 4.02 (d, J = 6.4 Hz, 1H), 3.14 (br s, 3H), 2.86 (s, 3H), 2.13−2.09 (m, 1H), 1.88 (t, J = 5.2 Hz, 1H), 1.41−1.39 (m, 1H). HRMS calculated for $C_{20}H_{21}N_6O_3S$ $(M + H)^+$, 425.1396; found, 425.1388.

*(1S,2R,3S,4R,5S)-4-(2-((5-Chlorothiophen-2-yl)ethynyl)-6-(methylamino)-9H-purin-9-yl)-2,3-dihydroxy-N-methylbicyclo[3.1.0]hexane-1-carboxamide (**33**).* Compound **33** (59%) was prepared from compound **40** following the same method for compound **22**. ^{1}H NMR (CD_3OD, 400 MHz) δ 8.11 (s, 1H), 7.31(d, J = 4.0 Hz, 1H), 7.03 (d, J = 4.0 Hz, 1H), 5.04 (d, J = 7.2 Hz, 1H), 4.86 (s, 1H), 4.01 (d, J = 6.8 Hz, 1H), 3.13 (br s, 3H), 2.86 (s, 3H), 2.12−2.09 (m, 1H), 1.88 (d, J = 4.8 Hz, 1H), 1.41−1.38 (m, 1H). HRMS calculated for $C_{20}H_{20}N_6O_3SCl$ $(M + H)^+$, 459.1006; found, 459.1005.

*(1S,2R,3S,4R,5S)-4-(2-((5-Bromothiophen-2-yl)ethynyl)-6-(methylamino)-9H-purin-9-yl)-2,3-dihydroxy-N-methylbicyclo[3.1.0]hexane-1-carboxamide (**34**).* Compound **34** (48%) was prepared from compound **40** following the same method for compound **22**. ^{1}H NMR (CD_3OD, 400 MHz) δ 8.10 (s, 1H), 7.28 (d, J = 4.0 Hz, 1H), 7.15 (d, J = 4.0 Hz, 1H), 5.05 (d, J = 5.2 Hz, 1H), 4.91 (s, 1H), 4.02 (d, J = 5.6 Hz, 1H), 3.14 (br s, 3H), 2.86 (s, 3H), 2.12−2.09 (m, 1H), 1.88 (t, J = 4.8 Hz, 1H), 1.41−1.37 (m, 1H). HRMS calculated for $C_{20}H_{20}N_6O_3SBr$ $(M + H)^+$, 503.0495; found, 503.0498.

*(1S,2S,3R,4R,5S)-2,3-dihydroxy-N-methyl-4-(6-(methylamino)-2-(thiazol-2-ylethynyl)-9H-purin-9-yl)bicyclo[3.1.0]hexane-1-carboxamide (**35**).* Compound **35** (64%) was prepared from compound **40** following the same method for compound **22**. ^{1}H NMR (CD_3OD, 400 MHz) δ 8.18 (s, 1H), 7.97 (d, J = 3.2 Hz, 1H), 7.82 (d, J = 3.2 Hz, 1H), 5.12 (d, J = 5.2 Hz, 1H), 4.90 (s, 1H), 4.04 (d, J = 6.4 Hz, 1H), 3.14 (br s, 3H), 2.86 (s, 3H), 2.11−2.07 (m, 1H), 1.86 (t, J = 4.8 Hz, 1H), 1.42−1.38 (m, 1H). HRMS calculated for $C_{19}H_{20}N_7O_3S$ $(M + H)^+$, 426.1343; found, 426.1342.

*(1S,2R,3S,4R,5S)-4-(2-((Ferrocen-yl)ethynyl)-6-(methylamino)-9H-purin-9-yl)-2,3-dihydroxy-N-methylbicyclo[3.1.0]hexane-1-carboxamide (**36**).* A solution of compound **40** (31 mg, 0.06 mmol) in methanol (3 mL) and 10% trifluoromethanesulfonic acid (2 mL) was heated at 70 °C for 5 h. Solvent was evaporated under vacuum, and the residue was purified on flash silica gel column chromatography (CH_2Cl_2:MeOH = 25:1) to give the isopropylidene-deblocked derivative (27 mg, 95%) as syrup. $PdCl_2(PPh_3)_2$ (8.5 mg, 0.012 mmol), CuI (1.1 mg, 0.006 mmol), ethynylferrocene (76.6 mg, 0.36 mmol), and triethylamine (0.08 mL, 0.6 mmol) were added to a solution of the obtained compound (27 mg, 0.06 mmol) in anhydrous DMF (1.2 mL), and the mixture stirred at room temperature overnight. Solvent was evaporated under vacuum, and the residue was purified on flash silica gel column chromatography (CH_2Cl_2:MeOH = 30:1) to give the compound **36** (29 mg, 86%) as light-yellow syrup. ^{1}H NMR (CD_3OD, 400 MHz) δ 8.10 (s, 1H), 5.01 (d, J = 6.4 Hz, 1H), 4.89 (s, 1H), 4.63 (s, 2H), 4.40 (s,2H), 4.31 (s, 6H), 4.01(d, J = 6.4 Hz, 1H), 3.15 (br s, 3H), 2.88 (s, 3H), 2.13−2.10 (m, 1H), 1.91 (t, J = 4.8 Hz, 1H), 1.42−1.38 (m, 1H). HRMS calculated for $C_{26}H_{27}N_6O_3Fe$ $(M + H)^+$, 527.1489; found, 527.1489.

*(1S,2R,3S,4R,5S)-4-(2-(Cyclopropylethynyl)-6-(methylamino)-9H-purin-9-yl)-2,3-dihydroxy-N-methylbicyclo[3.1.0]hexane-1-carboxamide (**37**).* Compound **37** (68%) was prepared from compound **40** following the same method for compound **22**. ^{1}H NMR (CD_3OD, 400 MHz) δ 8.06 (s, 1H), 5.02 (d, J = 6.0 Hz, 1H), 4.83 (s, 1H), 3.97 (d, J = 6.4 Hz, 1H), 3.10 (br s, 3H), 2.88 (s, 3H), 2.10−2.07 (m, 1H), 1.86 (t, J = 4.8 Hz, 1H), 1.59−1.52 (m, 1H), 1.40−1.37 (m, 1H), 1.00−0.98 (m, 2H), 0.94−0.86 (m, 2H). HRMS calculated for $C_{19}H_{23}N_6O_3$ $(M + H)^+$, 383.1832; found, 383.1838.

*(1S,2R,3S,4R,5S)-4-(2-(Cyclohexylethynyl)-6-(methylamino)-9H-purin-9-yl)-2,3-dihydroxy-N-methylbicyclo[3.1.0]hexane-1-carboxamide (**38**).* Compound **38** (71%) was prepared from compound **40** following the same method for compound **22**. ^{1}H NMR (CD_3OD, 400 MHz) δ 8.06 (s, 1H), 4.98 (d, J = 6.8 Hz, 1H), 4.85 (s, 1H), 3.95 (d, J = 6.4 Hz, 1H), 3.11 (br s, 3H) 2.86 (s, 3H), 2.86−2.62 (m, 1H), 2.11−2.08 (m, 1H), 1.99−1.96 (m, 2H), 1.89 (t, J = 4.8 Hz, 1H), 1.84−1.80 (m, 2H), 1.63−1.58 (m, 3H), 1.43−1.39 (m, 4H). HRMS calculated for $C_{22}H_{29}N_6O_3$ $(M + H)^+$, 425.2301; found, 425.2308.

Molecular Modeling. *hA_3AR and mA_3AR Homology Models.* Previously published homology models of the hA_3AR and mA_3AR,[11] built on the basis of a hybrid template structure using the homology modeling tool implemented in the MOE suite,[39] were used in this study. To build these models, an agonist-bound $hA_{2A}AR$ crystal structure (PDB code 3QAK)[27] was used as a template for the entire A_3AR structure except for the extracellular terminus of TM2 (residues from Val63 to Ser73 at the hA_3AR and from Val64 to Ser74 at the mA_3AR) and EL1 (residues from Leu74 to Tyr81 at the hA_3AR and from Leu75 to Tyr82 at the mA_3AR). The X-ray structure of the hβ_2 adrenergic receptor in

dx.doi.org/10.1021/jm501021n | J. Med. Chem. 2014, 57, 9901−9914

complex with the Gs protein (PDB code 3SN6),[40] after superimposition with the $hA_{2A}AR$ crystal structure, was used as template to build the extracellular terminus of TM2. No structural template was used for the modeling of EL1. Details of the modeling procedure have been previously described.[11,22]

Molecular Docking of (N)-Methanocarba Derivatives at A_3AR Models. Structures of compounds were built and prepared for docking using the build panel and the LigPrep panel implemented in the Schrödinger suite.[41] Molecular docking of the ligands at the A_3AR models was performed by means of the Glide[42] package part of the Schrödinger suite. The docking site was defined using key residues in the binding pocket of the A_3AR models, namely Phe (EL2), Asn (6.55), Trp (6.48), and His (7.43), and a 20 Å × 20 Å × 20 Å box was centered on these residues. Docking of ligands was performed in the rigid binding site using the XP (extra precision) procedure. The top scoring docking conformations of each ligand were subjected to visual inspection and analysis of protein−ligand interactions to select the final binding conformations.

Radioligand Binding Studies. [^{3}H]*R*-*N*^{6}-Phenylisopropyladenosine (**65**, [^{3}H]R-PIA, 63 Ci/mmol), [^{3}H](2-[*p*-(2-carboxyethyl)phenylethylamino]-5′-*N*-ethylcarboxamido-adenosine), (**66**, [^{3}H]CGS21680, 40.5 Ci/mmol), and [^{125}I]*N*^{6}-(4-amino-3-iodobenzyl)adenosine-5′-*N*-methyluronamide (**67**, [^{125}I]I-AB-MECA, 2200 Ci/mmol) were purchased from Perkin−Elmer Life and Analytical Science (Boston, MA). Test compounds were prepared as 5 mM stock solutions in DMSO and stored frozen. Pharmacological standards **2** (A_3AR agonist), adenosine-5′-*N*-ethylcarboxamide (**68**, NECA, nonselective AR agonist), and 2-chloro-*N*^{6}-cyclopentyladenosine (**69**, CCPA, A_1AR agonist) were purchased from Tocris R&D Systems (Minneapolis, MN).

Cell Culture and Membrane Preparation. CHO cells stably expressing the recombinant hA_1 and hA_3ARs and HEK293 cells stably expressing the $hA_{2A}AR$ were cultured in Dulbecco's Modified Eagle Medium (DMEM) and F12 (1:1) supplemented with 10% fetal bovine serum, 100 units/mL penicillin, 100 μg/mL streptomycin, and 2 μmol/mL glutamine. In addition, 800 μg/mL Geneticin was added to the A_{2A} media, while 500 μg/mL hygromycin was added to the A_1 and A_3 media. After harvesting, cells were homogenized and suspended in PBS. The suspension was homogenized and was then centrifuged at 1000*g* for 10 min. The pellet was discarded, and the suspension was recentrifuged at 20000*g* for 60 min at 4 °C. The resultant pellets were resuspended in Tris buffer, incubated with adenosine deaminase (3 units/mL) for 30 min at 37 °C. The suspension was homogenized with an electric homogenizer for 10 s, pipetted into 1 mL vials, and then stored at −80 °C until the binding experiments. The protein concentration was measured using the BCA Protein Assay Kit from Pierce Biotechnology, Inc. (Rockford, IL).[43]

Binding Assays. Into each tube in the binding assay was added 50 μL of increasing concentrations of the test ligand in Tris-HCl buffer (50 mM, pH 7.5) containing 10 mM $MgCl_2$, 50 μL of the appropriate agonist radioligand, and finally 100 μL of membrane suspension. For the A_1AR (22 μg of protein/tube), the radioligand used was [^{3}H]**65** (final concentration of 3.5 nM). For the $A_{2A}AR$ (20 μg/tube), the radioligand used was [^{3}H]**66** (10 nM). For the A_3AR (21 μg/tube), the radioligand used was [^{125}I]**67** (0.34 nM). Nonspecific binding was determined using a final concentration of 10 μM **68** diluted with the buffer. The mixtures were incubated at 25 °C for 60 min in a shaking water bath. Binding reactions were terminated by filtration through Brandel GF/B filters under a reduced pressure using a M-24 cell harvester (Brandel, Gaithersburg, MD). Filters were washed three times with 3 mL of 50 mM ice-cold Tris-HCl buffer (pH 7.5). Filters for A_1 and $A_{2A}AR$ binding were placed in scintillation vials containing 5 mL of Hydrofluor scintillation buffer and counted using a PerkinElmer liquid scintillation analyzer (Tri-Carb 2810TR). Filters for A_3AR binding were counted using a Packard Cobra II γ-counter. The K_i values were determined using GraphPad Prism for all assays.

Similar competition binding assays were conducted using HEK293 cell membranes expressing mARs using [^{125}I]**67** to label A_1 or A_3ARs and [^{3}H]**65** to label $A_{2A}ARs$. IC_{50} values were converted to K_i values as described.[44] Nonspecific binding was determined in the presence of 100 μM **68**.

Cyclic AMP Accumulation Assay. Cyclic AMP assays were conducted with HEK293 cells expressing the mA_3AR. HEK293 cells were detached from cell culture plates, resuspended in serum-free DMEM containing 25 mM HEPES (pH 7.4), 1 unit/mL adenosine deaminase, 4-(3-butoxy-4-methoxyphenyl)methyl-2-imidazolidone (Tocris, Ro 20,1724, 20 μM) and 300 nM 8-[4-[4-(4-chlorophenzyl)piperazide-1-sulfonyl)phenyl]]-1-propylxanthine (Tocris, PSB603, 300 nM, to inhibit $A_{2B}ARs$ expressed endogenously in HEK293 cells), and then transferred to polypropylene tubes (2×10^5 cells/tube). The cells were coincubated with forskolin (10 μM) and AR ligands for 15 min at 37 °C with shaking, after which the assays were terminated by adding 500 μL of 1 N HCl. The lysates were centrifuged at 4000*g* for 10 min. The cyclic AMP concentration was determined in the supernatants using a competitive binding assay, as previously described.[45] EC_{50} and E_{max} values were calculated by fitting the data to $E = E_{min} + (E_{max} - E_{min})/(1 + 10^{x-\log EC50})$.

In Vivo Studies of Neuropathic Pain. Methods are the same as those reported and are briefly summarized here.[10,11]

Experimental Animals. Male CD-1 mice (25−30 g) from Harlan (Indianapolis, IN) were housed 4−5 (for mice) per cage in a controlled environment (12 h light/dark cycles) with food and water available ad libitum. Experiments were performed in accordance with International Association for the Study of Pain, NIH guidelines on laboratory animal welfare, and Saint Louis University Institutional Animal Care and Use Committee recommendations. Experimenters were blinded to treatment conditions in all experiments.

CCI Model of Neuropathic Pain. CCI to the sciatic nerve of the left hind leg in mice was performed under general anesthesia using the well characterized Bennett model.[25] Briefly, mice (weighing 25−30 g at the time of surgery) were anesthetized with 3% isoflurane/100% O_2 inhalation and maintained on 2% isoflurane/100% O_2 for the duration of surgery. The left thigh was shaved and scrubbed with Nolvasan (Zoetis, Madison, NJ), and a small incision (1−1.5 cm in length) was made in the middle of the lateral aspect of the left thigh to expose the sciatic nerve. The nerve was loosely ligated around the entire diameter of the nerve at three distinct sites (spaced 1 mm apart) using silk sutures (6.0). The surgical site was closed with a single muscle suture and a skin clip. Pilot studies established that under our experimental conditions peak mechano-allodynia develops by D5−D7 following CCI. Test substances or their vehicles were administered as 3 μmol/kg doses given by gavage (0.2 mL po) at peak mechano-allodynia (D7). The vehicle used consisted of 10% DMSO in 0.5% methylcellulose (diluted from a 5 mM stock solution in DMSO). Methylcellulose (lot no. 021M0067V) was obtained from Sigma viscosity 400 cP and prepared in sterile distilled water (UPS).

Statistical Analysis for in Vivo Experiments. Data are expressed as mean ± SEM for *n* animals. Behavioral data were analyzed by two-way ANOVA with Bonferroni comparisons. Significant differences were defined at a $P < 0.05$. All statistical analysis was performed using GraphPad Prism (v5.03, GraphPad Software, Inc., San Diego, CA).

Binding to Off-Target Sites. K_i determinations and binding profiles in a broad screen of receptors and channels were generously provided by the National Institute of Mental Health's Psychoactive Drug Screening Program, contract no. HHSN-271-2008-00025-C (NIMH PDSP). The NIMH PDSP is Directed by Bryan L. Roth MD, Ph.D. at the University of North Carolina at Chapel Hill and Project Officer Jamie Driscol at NIMH, Bethesda MD, USA. For experimental details, please refer to the PDSP web site http://pdsp.med.unc.edu/ and click on "Binding Assay" or "Functional Assay" on the menu bar.

■ ASSOCIATED CONTENT

Supporting Information

NMR and mass spectra of selected synthesized compounds, results of PDSP screening and 3D coordinates of the modeled hA_3AR and mA_3AR complexes with **33** (PDB), procedures for in vitro ADME measurements. This material is available free of charge via the Internet at http://pubs.acs.org.

AUTHOR INFORMATION

Corresponding Author

*Phone: 301-496-9024. Fax: 301-496-8422. E-mail: kajacobs@helix.nih.gov.

Notes

The authors declare no competing financial interest.

ACKNOWLEDGMENTS

We thank Dr. John Lloyd and Dr. Noel Whittaker (NIDDK) for mass spectral determinations. This research was supported by the National Institutes of Health (Intramural Research Program of the NIDDK and R01HL077707). We thank Dr. Bryan L. Roth (University of North Carolina at Chapel Hill) and National Institute of Mental Health's Psychoactive Drug Screening Program (contract no. HHSN-271-2008-00025-C) for screening data.

ABBREVIATIONS USED

AR, adenosine receptor; cAMP, adenosine 3′,5′-cyclic monophosphate; CCI, chronic constriction injury; CHO, Chinese hamster ovary; CNS, central nervous system; CYP, cytochrome P450; DMEM, Dulbecco's Modified Eagle Medium; DMF, *N*,*N*-dimethylformamide; EL, extracellular loop; GPCR, G protein-coupled receptor; HEPES, 2-[4-(2-hydroxyethyl)piperazin-1-yl]-ethanesulfonic acid; HEK, human embryonic kidney; HRMS, high resolution mass spectroscopy; NECA, 5′-*N*-ethylcarboxamidoadenosine; NMR, nuclear magnetic resonance; PBS, phosphate buffered saline; PBR, peripheral benzodiazepine receptor; PWT, paw withdrawal threshold; RMS, root-mean-square; SAR, structure−affinity relationship; TBAP, tetrabutylammonium dihydrogen phosphate; TEA, triethylamine; TM, transmembrane helix; tPSA, total polar surface area; MW, molecular weight

REFERENCES

(1) Renfrey, S.; Downton, C.; Featherstone, J. The painful reality. *Nature Rev. Drug Discovery* **2003**, *2*, 175−176.

(2) Farquhar-Smith, P. Chemotherapy-induced neuropathic pain. *Curr. Opin. Supportive Palliative Care* **2011**, *5*, 1−7.

(3) Ossipov, M. H.; Lai, J.; King, T.; Vanderah, T. W.; Malan, T. P.; Hruby, V. J.; Porreca, F. Antinociceptive and nociceptive actions of opioids. *J. Neurobiol.* **2004**, *61*, 126−148.

(4) Zylka, M. J. Pain-relieving prospects for adenosine receptors and ectonucleotidases. *Trends Mol. Med.* **2011**, *17*, 188−196.

(5) Boison, D. Adenosine kinase: exploitation for therapeutic gain. *Pharmacol. Rev.* **2013**, *65*, 906−943.

(6) Little, J. W; Ford, A.; Symons-Liguori, A. M.; Chen, Z.; Janes, K.; Doyle, T.; Xie, J.; Luongo, L.; Tosh, D. K.; Maione, S.; Bannister, K.; Dickenson, A.; Vanderah, T. W.; Porreca, F.; Jacobson, K. A.; Salvemini, D. Endogenous adenosine A_3 receptor activation selectively alleviates persistent pain states. *Brain* **2015**, DOI: 10.1093/brain/awu330.

(7) Tchilibon, S.; Kim, S. K.; Gao, Z. G.; Harris, B. A.; Blaustein, J.; Gross, A. S.; Melman, N.; Jacobson, K. A. Exploring distal regions of the A_3 adenosine receptor binding site: sterically-constrained N^6-(2-phenylethyl)adenosine derivatives as potent ligands. *Bioorg. Med. Chem.* **2004**, *12*, 2021−2034.

(8) Yaar, R.; Lamperti, E. D.; Toselli, P. A.; Ravid, K. Activity of the A_3 adenosine receptor gene promoter in transgenic mice: characterization of previously unidentified sites of expression. *FEBS Lett.* **2002**, *532*, 267−272.

(9) Fishman, P.; Bar-Yehuda, S.; Liang, B. T.; Jacobson, K. A. Pharmacological and therapeutic effects of A_3 adenosine receptor (A_3AR) agonists. *Drug Discovery Today* **2012**, *17*, 359−366.

(10) Chen, Z.; Janes, K.; Chen, C.; Doyle, T.; Tosh, D. K.; Jacobson, K. A.; Salvemini, D. Controlling murine and rat chronic pain through A_3 adenosine receptor activation. *FASEB J.* **2012**, *26*, 1855−1865.

(11) Paoletta, S.; Tosh, D. K.; Finley, A.; Gizewski, E.; Moss, S. M.; Gao, Z. G.; Auchampach, J. A.; Salvemini, D.; Jacobson, K. A. Rational design of sulfonated A_3 adenosine receptor-selective nucleosides as pharmacological tools to study chronic neuropathic pain. *J. Med. Chem.* **2013**, *56*, 5949−5963.

(12) Jeong, L. S.; Lee, H. W.; Jacobson, K. A.; Kim, H. O.; Shin, D. H.; Lee, J. A.; Gao, Z. G.; Lu, C.; Duong, H. T.; Gunaga, P.; Lee, S. K.; Jin, D. Z.; Chun, M. W.; Moon, H. R. Structure−activity relationships of 2-chloro-N^6-substituted-4′-thioadenosine-5′-uronamides as highly potent and selective agonists at the human A_3 adenosine receptor. *J. Med. Chem.* **2006**, *49*, 273−281.

(13) David, M.; Akerman, L.; Ziv, M.; Kadurina, M.; Gospodinov, D.; Pavlotsky, F.; Yankova, R.; Kouzeva, V.; Ramon, M.; Silverman, M. H.; Fishman, P. Treatment of plaque-type psoriasis with oral CF101: data from an exploratory randomized phase 2 clinical trial. *J. Eur. Acad. Dermatol. Venereol.* **2012**, *26*, 361−367.

(14) Stemmer, S. M.; Benjaminov, O.; Medalia, G.; Ciuraru, N. B.; Silverman, M. H.; Bar-Yehuda, S.; Fishman, S.; Harpaz, Z.; Farbstein, M.; Cohen, S.; Patoka, R.; Singer, B.; Kerns, W. D.; Fishman, P. CF102 for the treatment of hepatocellular carcinoma: a phase I/II, open-label, dose-escalation study. *Oncologist* **2013**, *18*, 25−26.

(15) Janes, K.; Wahlman, C.; Little, J.; Doyle, T.; Tosh, D.; Jacobson, K.; Salvemini, D. Spinal neuroimmmune activation is independent of T-cell infiltration and attenuated by A_3 adenosine receptor agonists in a model of oxaliplatin-induced peripheral neuropathy. *Brain, Behav., Immun.*, **2014**, http://dx.doi.org/10.1016/j.bbi.2014.08.010.

(16) Janes, K.; Esposito, E.; Doyle, T.; Cuzzocrea, S.; Tosh, D.; Jacobson, K.; Salvemini, D. A_3 adenosine receptor agonists prevent the development of paclitaxel-induced neuropathic pain by modulating spinal glial-restricted redox-dependent signaling pathways. *Pain*, **2014**, *155*, 2560−2567.

(17) Chen, J. F.; Eltzschig, H. K.; Fredholm, B. B. Adenosine receptors as drug targets—what are the challenges? *Nature Rev. Drug Discovery* **2013**, *12*, 265−286.

(18) Luongo, L.; Petrelli, R.; Gatta, L.; Giordano, C.; Guida, F.; Vita, P.; Franchetti, P.; Grifantini, M.; de Novellis, V.; Cappellacci, L.; Malone, S. 5′-Chloro-5′-deoxy-(±)-ENBA, a potent and selective adenosine A_1 receptor agonist, alleviates neuropathic pain in mice through functional glial and microglial changes without affecting motor or cardiovascular functions. *Molecules* **2012**, *17*, 13712−13726.

(19) Mantell, S.; Jones, R.; Trevethick, M. Design and application of locally delivered agonists of the adenosine A_{2A} receptor. *Expert Rev. Clin. Pharmacol.* **2010**, *3*, 55−72.

(20) Jacobson, K. A.; Kim, H. O.; Siddiqi, S. M.; Olah, M. E.; Stiles, G. L.; von Lubitz, D. K. J. E. A_3 adenosine receptors: design of selective ligands and therapeutic prospects. *Drugs Future* **1995**, *20*, 689−699.

(21) Yang, J. N.; Wang, Y.; Garcia-Roves, P. M.; Björnholm, M.; Fredholm, B. B. Adenosine A_3 receptors regulate heart rate, motor activity and body temperature. *Acta Physiol.* **2010**, *199*, 221−230.

(22) Tosh, D. K.; Deflorian, F.; Phan, K.; Gao, Z. G.; Wan, T. C.; Gizewski, E.; Auchampach, J. A.; Jacobson, K. A. Structure-guided design of A_3 adenosine receptor-selective nucleosides: combination of 2-arylethynyl and bicyclo[3.1.0]hexane substitutions. *J. Med. Chem.* **2012**, *55*, 4847−4860.

(23) Leeson, P. D.; Springthorpe, B. The influence of drug-like concepts on decision-making in medicinal chemistry. *Nature Rev. Drug Discovery* **2007**, *6*, 881−890 DOI: 10.1038/nrd2445.

(24) Lee, J. A.; Berg, E. L. Neoclassic drug discovery: the case for lead generation using phenotypic and functional approaches. *J. Biomol. Screening* **2013**, *18*, 1143−1155.

(25) Bennett, G. J.; Xie, Y. K. A peripheral mononeuropathy in rat that produces disorders of pain sensation like those seen in man. *Pain* **1988**, *33*, 87−107.

(26) Jensen, N. H.; Roth, B. L. Massively parallel screening of the receptorome. *Comb. Chem. High Throughput Screening* **2008**, *11*, 420−426.

(27) Xu, F.; Wu, H.; Katritch, V.; Han, G. W.; Jacobson, K. A.; Gao, Z. G.; Cherezov, V.; Stevens, R. Agonist bound structure of the human adenosine A_{2A} receptor. *Science* **2011**, *332*, 322−327.

(28) Lebon, G.; Warne, T.; Edwards, P. C.; Bennett, K.; Langmead, C. J.; Leslie, A. G.; Tate, C. G. Agonist-bound adenosine A_{2A} receptor structures reveal common features of GPCR activation. *Nature* **2011**, *474*, 521−525.
(29) Tosh, D. K.; Jacobson, K. A. Methanocarba ring as a ribose modification in ligands of G protein-coupled purine and pyrimidine receptors: Synthetic approaches. *MedChemComm* **2013**, *4*, 619−630.
(30) Paoletta, S.; Tosh, D. K.; Salvemini, D.; Jacobson, K. A. Structural probing of off-target G protein-coupled receptor activities within a series of adenosine/adenine congeners. *PLoS One* **2014**, *9*, e97858.
(31) Swinney, D. C.; Anthony, J. How were new medicines discovered? *Nature Rev. Drug Discovery* **2011**, *10*, 507−519.
(32) Kirk, K. L. Selective fluorination in drug design and development: an overview of biochemical rationales. *Curr. Top. Med. Chem.* **2006**, *6*, 1447−1456.
(33) Ferreira, S. B.; Kaiser, C. R. Pyrazine derivatives: a patent review (2008−present). *Expert Opin. Ther. Pat.* **2012**, *22*, 1033−1051.
(34) Lang, D.; Freudenberger, C.; Weinz, C. In vitro metabolism of rivaroxaban, an oral, direct Factor Xa inhibitor, in liver microsomes and hepatocytes of rats, dogs, and humans. *Drug Metab. Dispos.* **2009**, *37*, 1046−1055.
(35) Gasser, G.; Metzler-Nolte, N. The potential of organometallic complexes in medicinal chemistry. *Curr. Opin. Chem. Biol.* **2012**, *16*, 84−91.
(36) Paira, P.; Chow, M. J.; Venkatesan, G.; Kosaraju, V. K.; Cheong, S. L.; Klotz, K. N.; Ang, W. H.; Pastorin, G. Organoruthenium antagonists of human A_3 adenosine receptors. *Chem.—Eur. J.* **2013**, *19*, 1521−3765.
(37) Dal Ben, D.; Buccioni, M.; Lambertucci, C.; Marucci, G.; Volpini, R.; Cristalli, G. The importance of alkynyl chain presence for the activity of adenine nucleosides/nucleotides on purinergic receptors. *Curr. Med. Chem.* **2011**, *18*, 1444−1463.
(38) Dansette, P. M.; Bertho, G.; Mansuy, D. First evidence that cytochrome P450 may catalyze both S-oxidation and epoxidation of thiophene derivatives. *Biochem. Biophys. Res. Commun.* **2005**, *338*, 450−455.
(39) *Molecular Operating Environment (MOE)*, version 2012.10; Chemical Computing Group Inc.: 1255 University St., Suite 1600, Montreal, QC H3B 3X3, Canada, 2012.
(40) Rasmussen, S. G. F.; DeVree, B. T.; Zou, Y.; Kruse, A. C.; Chung, K. Y.; Kobilka, T. S.; Thian, F. S.; Chae, P. S.; Pardon, E.; Calinski, D.; Mathiesen, J. M.; Shah, S. T. A.; Lyons, J. A.; Caffrey, M.; Gellman, S. H.; Steyaert, J.; Skiniotis, G.; Weis, W. I.; Sunahara, R. K.; Kobilka, B. K. Crystal structure of the β_2 adrenergic receptor−Gs protein complex. *Nature* **2011**, *477*, 549−555.
(41) *Schrödinger Suite 2012*; Schrödinger, LLC: New York, 2012.
(42) Friesner, R. A.; Banks, J. L.; Murphy, R. B.; Halgren, T. A.; Klicic, J. J.; Mainz, D. T.; Repasky, M. P.; Knoll, E. H.; Shaw, D. E.; Shelley, M.; Perry, J. K.; Francis, P.; Shenkin, P. S. Glide: a new approach for rapid, accurate docking and scoring. 1. Method and assessment of docking accuracy. *J. Med. Chem.* **2004**, *47*, 1739−1749.
(43) Bradford, M. M. A rapid and sensitive method for the quantitation of microgram quantities of protein utilizing the principle of protein−dye binding. *Anal. Biochem.* **1976**, *72*, 248−254.
(44) Cheng, Y. C.; Prusoff, W. H. Relationship between inhibition constant (K1) and concentration of inhibitor which causes 50% inhibition (I50) of an enzymatic reaction. *Biochem. Pharmacol.* **1973**, *22*, 3099−3108.
(45) Nordstedt, C.; Fredholm, B. B. A modification of a protein-binding method for rapid quantification of cAMP in cell-culture supernatants and body fluid. *Anal. Biochem.* **1990**, *189*, 231−234.
(46) Ballesteros, J. A.; Weinstein, H. Integrated methods for the construction of three dimensional models and computational probing of structure-function relationships in G-protein coupled receptors. *Methods Neurosci.* **1995**, *25*, 366−428.